Funded by the European Union

Horizon Europe

EUROPEAN COMMISSION European Climate, Infrastructure and Environment Executive Agency (CINEA)

Grant agreement no. 101056765

Electric Vehicles Management for carbon neutrality in Europe

Deliverable D9.4
Demonstration results report for the Danish demo

Document Details

Due date	28-02-2026
Actual delivery date	10-03-2026
Lead Contractor	DTU
Version	1.0
Prepared by	Xihai Cao (DTU), Mathilde Roblot (DTU), Simone Striani (DTU), Kristoffer Laust Pedersen (DTU), Francesco Pastorelli (DTU), Pietro Zunino (DTU), Anna Malkova (DTU), Jan Engelhardt (DTU), Haris Ziras (DTU), Mattia Marinelli (DTU)
Reviewed by	Célia Jesus (INESC ID) & Evangelos Karfopoulos (PPC)
Dissemination Level	Public

Project Contractual Details

Project Title	Electric Vehicles Management for carbon neutrality in Europe
Project Acronym	EV4EU
Grant Agreement No.	101056765
Project Start Date	01-06-2022
Project End Date	31-05-2026
Duration	48 months

Document History

Version	Date	Contributor(s)	Description
0.1	14/09/2025	DTU	Draft
0.2	23/02/2026	DTU	Version for revision
1.0	03/03/2026	DTU	Final version

Disclaimer

Acknowledgment

This document is a deliverable of EV4EU project. EV4EU has received funding from the European Union´s Horizon Europe programme under grant agreement no. 101056765.

Funded by
the European Union

[1] https://ev4eu.eu/

Executive Summary

Deliverable 9.4 represents a significant milestone for our project, showcasing the experimental results gathered from two smart electric vehicles (EV) charging demonstration sites: the DTU Risø campus in Roskilde and Campus Bornholm in Rønne on Bornholm Island. At each site, commercially available EVs were connected to chargers equipped with our innovative distributed control architecture, and extensive measurement campaigns were conducted to validate system performance under real-world conditions.

Central to this deliverable is a two-layer control architecture. The local control layer, embedded directly within each charger, prioritizes charging sessions according to user's urgency. Simultaneously, the global control layer, hosted on a cloud server, dynamically adjusts and coordinates power consumption across multiple EV parking areas. Both layers communicate via a robust network of microcontrollers and servers, ensuring seamless and low-latency exchanges of measurements and control setpoints. This integrated control architecture effectively links smart EV chargers with local renewable energy sources, specifically building-integrated photovoltaic panels and two small-scale wind turbines.

Supporting these control functions is a comprehensive data logging and management system. Each charger, as well as the point of common coupling (PCC), is equipped with a smart meter that records crucial operational data—power measurements, session priorities, and command acknowledgments, and securely transmits this data to a centralized database hosted at energydata.dk. This centralized repository serves both current and future research needs. Additionally, real-time operational monitoring is enabled through dedicated dashboards accessible at evchargersrisoe.windenergy.dtu.dk and evchargersbornholm.windenergy.dtu.dk. This structured data architecture lays the groundwork for detailed performance analysis and future scalability.

This document presents results from both the demonstration of charger functionalities and the analysis of key performance indicators (KPIs) regarding user charging behavior at the two demonstration sites. Initial results confirm the system's ability to provide flexibility services without compromising individual user requirements. Specifically, functionalities such as frequency regulation, renewable energy following, power sharing, and power scheduling demonstrated high accuracy and timeliness. The findings also provided valuable insights into the constraints experienced by different EV models when subjected to certain control actions. Furthermore, data analysis reveals insights into user charging behaviors, the flexibility potential of parking areas for various flexibility services, consumption profiles, and charging costs integrating local renewable energy production.

In summary, Deliverable 9.4 validates the feasibility and operational effectiveness of our distributed EV charging architecture, from control logic and data management to real-world validation, establishing a robust foundation for future deployments and ongoing system optimization.

Table of Contents

Executive Summary 4
Table of Contents 5
List of Figures 6
Acronyms 7
1 Introduction 8
1.1 Scope and Objectives 8
1.2 Structure 9
2 Design and implementation of the architecture 10
2.1 The demo sites 10
2.2 The general concept of architecture 11
2.3 The Cloud Aggregator 12
2.3.1 Frequency Regulation Mode: 13
2.3.2 RES mode: 13
2.4 The Virtual Aggregator 14
2.4.1 Normal mode 14
2.4.2 Phase balancing mode 17
2.5 Implementation of architecture 18
3 Controllers validation in real conditions and lab demonstration 21
3.1 Transformer Protection 21
3.2 Frequency regulation mode 22
3.3 Scheduling and priority 24
3.4 RES following mode 25
3.5 Phase balancing mode 26
4 Key Performance Indicators (KPIs) 29
4.1 Technical KPIs 29
4.2 Economic KPIs 35
4.3 User related KPIs 37
5 Conclusions 42
6 References 43

List of Figures

Figure 1: Location of the two demonstration sites. 10
Figure 2: picture of one of the chargers installed in Risø campus 11
Figure 3: Global system architecture and communication paths between different actors. 12
Figure 4: Simplified block diagram of the system performing frequency regulation. 13
Figure 5: Simplified block diagram of the system performing RES following mode. 14
Figure 6: Flowchart of the State Machine describing every state and their conditions. 15
Figure 7: Complete block diagram of the architecture of the system. 19
Figure 8: Beagle bones for the VAs of three chargers and the CA 20
Figure 9: Active power of EVs (top plot) and at transformer (bottom plot) in the TRAFO 22
Figure 10: Frequency regulation time history. The graph below is a zoomed instance of the above graph for better time visualization. The blue lines illustrate the frequency while the red lines illustrate the Power utilized by the cluster. 23
Figure 11: Time history of the priority of the two EVs during the frequency test. 23
Figure 12: time history of the individual EV power consumption (bottom figure) 24
Figure 13: Power scheduling between two EVs. 25
Figure 14: Priority trend during the power scheduling test. 25
Figure 15: Power consumption and power measurement at the PCC for the parking lot during RES following mode 26
Figure 16: time series of the experiment. The top three graphs show the power consumption over time for each EV while the bottom three graph show the power reference from the CA in dark green, in bright green, purple and consumption 27
Figure 17: Recording charging entries in Risø and Bornholm parking lots 29
Figure 18: Online period of the chargers in Risø and Bornholm parking lots 30
Figure 19: Average active power, power factor and number of EVs charging in Risø and Bornholm parking lots 31
Figure 20: Flexibility indices of Risø parking lot 33
Figure 21: Daily average energy accumulated in the EVs 33
Figure 22: Monthly average charging success ratio in Risø and Bornholm parking lots 34
Figure 23: Time delays and the correlation at the PCC between the detection of a triggering event and the full response of the parking lot. 35
Figure 24: Cost of energy with and without accounting for the self-consumption from PV in Risø and Bornholm parking lots. 36
Figure 25: Average number of EVs connected and charging during the work week in Risø parking lot 38
Figure 26: Hourly distribution of the arrival and departure time in Risø parking lot 38
Figure 27: Distribution of the averaged amount of energy charged per session in Risø parking lot 39

Acronyms

AC	Alternating current
ACDC	Autonomously Controlled Distributed Chargers project, financed by EUDP
AWS	Amazon Web Services
BB	Beagle bone microcontrollers
BUC	Business Use Case
CA	Cloud Aggregator
CO2	Carbon dioxide
CPO	Charging Point Operator
DR	Demand Response
DSO	Distribution System Operator
DTU	Technical University of Denmark
EV	Electric Vehicle
FCR-N	Frequency Containment Reserve - Normal operation
I	Current
ICT	Information and communication technology
ID	Identification
KPI	Key Performance Indicator
kW	Kilowatt
Log	file that captures events
ρ	priority
P	Active power
PCC	Point of Common Coupling
PV	Photovoltaics
S	Apparent power
t	time
UC	Use Case
V	Voltage
V1G	Smart Charging
V2B	Vehicle to Building
V2G	Vehicle to Grid
V2X	Vehicle to Everything
VA	Virtual Aggregator
Viz script	Visualization script written in Python
WB	custom-made whiteboard
WP	Work Package

1 Introduction

Governments are actively promoting the shift from fossil fuels to sustainable technologies, prioritizing renewable energy sources (RES) for electricity production and electric vehicles (EVs) for transportation to reduce CO_2 emissions. However, integrating RES into power systems poses challenges due to their intermittent and unpredictable nature, increasing the need for flexible energy solutions to balance supply and demand. Traditionally, grid stability has been managed through flexibility markets, but the rise of RES demands new approaches to handle the volatility.

Smart EV charging represents a viable solution by turning chargers into flexible grid assets, offering significant storage capacity and stability to future smart grids. Charging clusters, managed by charging point operators (CPOs) and aggregators, adjust EV charging power to prevent grid overload and provide flexibility services. Participating in these flexibility markets can benefit stakeholders financially by generating revenue for operators and lowering costs for users.

Despite its benefits, smart charging faces technical, economic, and regulatory barriers that limit investment and EV adoption. Addressing these challenges requires coordinated efforts among industry stakeholders and policymakers to standardize and incentivize infrastructure development. CPOs face uncertainties regarding the profitability and flexibility potential of smart EV clusters, necessitating careful planning and strategic placement of infrastructure, alongside developing robust control strategies and user-friendly communication systems.

Future research should prioritize developing, testing, and optimizing smart charging strategies at various scales, from large-scale analyses that guide strategic placement of EV clusters in urban environments, to smaller-scale optimizations enhancing flexibility and grid compatibility based on specific usage patterns.

1.1 Scope and Objectives

In this context, the focus of this deliverable is to demonstrate and evaluate the distributed control architecture for smart electric vehicle charging developed under the EV4EU project. The demonstration and evaluation have been conducted at two Danish sites: the DTU Risø campus and Campus Bornholm, with a particular emphasis on assessing the architecture's capability to deliver grid flexibility services effectively.

Specifically, the objectives of this deliverable are fourfold.

First, it provides a comprehensive description of the distributed control architecture, detailing its design, controller implementations, data structures, and the specific hardware and software deployed at the demonstration sites.

Second, it showcases the performance and practical application of this architecture, both in controlled laboratory conditions and through real-world deployment at the demonstration sites. This involves demonstrating core charging functionalities such as power-sharing, power-scheduling, and prioritization mechanisms, alongside advanced flexibility services including frequency regulation and alignment with renewable energy production.

Third, the deliverable analyses extensive metering data collected through advanced monitoring and data-logging systems to reveal insights into long-term user charging behaviors and performance metrics observed during the demonstration period.

Finally, the deliverable identifies and characterizes the operational limitations, as well as the flexibility potential, of commercially available EV chargers when utilized as flexible loads within broader energy management frameworks. This assessment supports further development and optimization of smart charging solutions within the evolving landscape of grid management.

1.2 Structure

Section 1 – Introduction
This section introduces Deliverable 9.4 and outlines its scope and objectives, focusing on the demonstration and evaluation of the distributed control architecture for smart EV charging developed within the EV4EU project.

Section 2– Design and Implementation of the architecture
This section begins with an overview of the two demonstration sites, DTU Risø campus and Campus Bornholm, and then presents a general description of the distributed control architecture. It continues with detailed accounts of the global and local controller designs and explains the overall control and communication framework.

Section 3– Controllers validation in real conditions and lab demonstration
This section analyses the system's advanced charging functions—power-scheduling, power-sharing, and charging prioritization—and reports on performance tests in frequency regulation mode, renewable-energy-following mode, phase balancing control, and charging optimization based on RES production and electricity prices.

Section 4 – Key Performance Indicators (KPIs)
This section examines the data logs collected throughout 2025 at both demonstration sites. It presents key performance indicators on user charging behavior, charging costs, system robustness, and the parking lots' flexibility potential.

Section 5 – Conclusions
This final section summarizes the work presented in this document, draws conclusions on the technology's potential, and offers reflections on future research opportunities using these demonstration sites.

2 Design and implementation of the architecture

2.1 The demo sites

To continue the experimental demonstration of the distributed control architecture, two identical EV charging systems were installed—one at DTU's Risø research campus and one at Campus Bornholm. Each system occupies a parking lot (shown in Figure 1) and comprises six AC chargers, each rated for 32 A (22 kW on three phases) with two outlets apiece, allowing up to 12 vehicles to charge simultaneously. Both installations share a single 63 A (43 kW three-phase) grid connection and tie into the grid via an on-site electrical cabinet that serves as the point of common coupling (PCC). Figure 2 shows one of the chargers installed at the Risø campus.

Figure 1: Location of the two demonstration sites.

The charging clusters are integrated within the SYSLAB smart energy system lab, which consists of an internal grid within the Risø campus including distributed units for both production (such as wind turbines and PVs), consumption (building loads and controllable loads), and energy storage (battery technologies or supercapacitors). SYSLAB also consists of data centres, where the system can be

Figure 2: picture of one of the chargers installed in Risø campus

completely monitored and controlled. Moreover, each device in such internal grid at each node is constantly storing datasets useful for the post processing and studying of the results. Although the charging cluster at campus Bornholm is not physically connected to the SYSLAB grid, the control architecture controls it as a SYSLAB unit, providing freedom of controlling the cluster using inputs that includes the ones from the SYSLAB grid.

2.2 The general concept of architecture

In this paragraph the model and the distributed control architecture developed is described. Figure 3 provides an overview of the control architecture. In the figure the grey shaded areas represent a number N of generic location in the distribution grid. The electricity in each area is distributed to all the connected buildings, and to the parking lots. The Cloud Aggregator (CA) performs cloud-based global control. The Virtual Aggregator (VA), presented in all the chargers of the N parking lots, performs local control. The functions of the CA are the following: signal reception and processing, controllability and power set point dispatch. The CA receives signals from the grid, such as RES production from the surrounding RES power plants, and grid congestion. The CA provides controllability to different actors (Aggregator, DSOs and TSO) according to other signals (for example electricity price, or market bids). In addition, the CA provides information to parking lot users about which parking lots are available via mobile app. Users can also input different requests through the app to schedule and set their charging session priority. The users' inputs are expected energy to be charged and the scheduled time of departure. The CA processes these inputs and dispatches to the VA both power set points and user requests.

The VA receives inputs from the CA and from the smart meter of the parking lot. On the one hand, the VA stores the user's information and schedules the charging sessions accordingly. Based on user preferences, the VA gives instructions to the chargers, such as charging priority and power scheduling based on energy charged. On the other hand, the VA of each parking lot matches the power reference given by the CA with the actual consumption recorded from the smart meter. In case there are buildings connected to the same smart meter, the VA will additionally perform power sharing between the buildings and the parking lot. For each time-step, the VA broadcasts new power set points to all the chargers of its cluster.

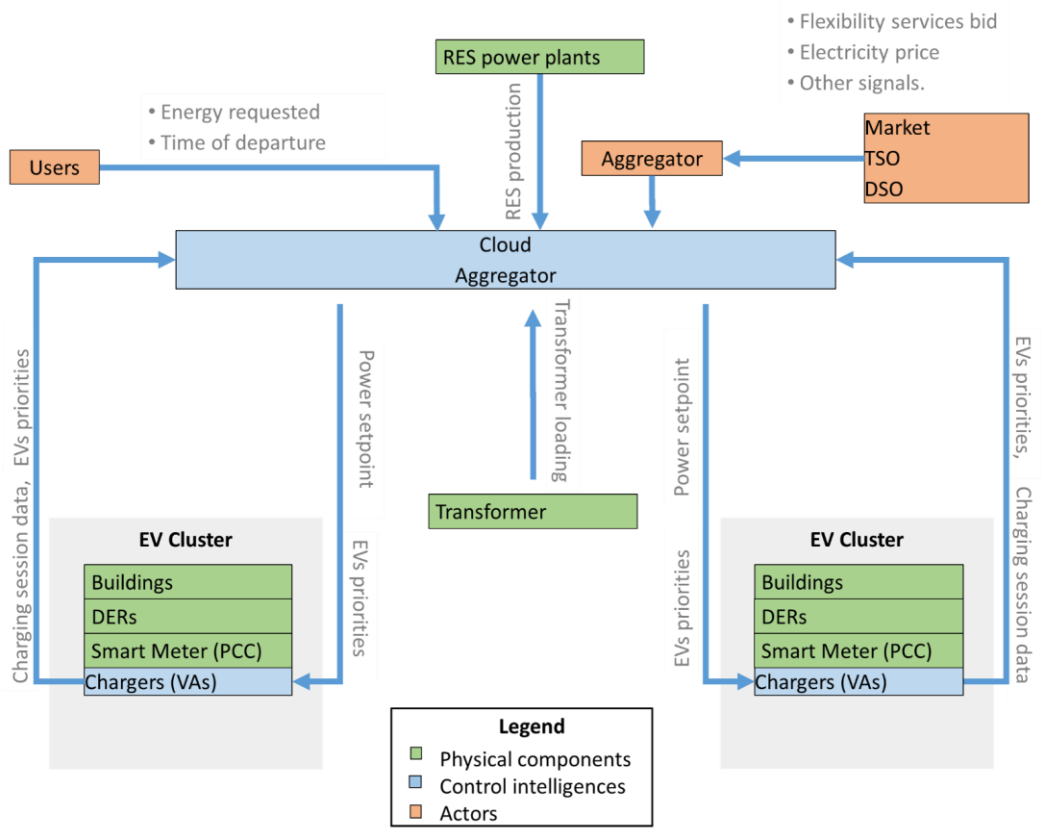

Figure 3: Global system architecture and communication paths between different actors.

Global control ends each iteration with a feedback loop from the smart meter to the CA. The smart meter updates the CA on the power consumed in the previous iteration. Therefore, the CA collects power consumption data from the N parking lots and redistributes the power among the parking lots according to the availability of cars and local grid conditions.

2.3 The Cloud Aggregator

The distributed control concept offers a double-layer control: The high-level control of the cluster is performed by the cloud aggregator (CA), a computational intelligence located in a cloud server; The autonomous control of each charger is managed by the virtual aggregator (VA) embedded within each charger. The cluster of chargers is connected to the grid at the point of common coupling (PCC) where their consumption and grid conditions are read via a smart meter. The meter provides measurements of frequency and consumed power at the PCC, which are read by the CA and the VAs, respectively. A user interface allows users to input the energy requested, and the departure time for the charging session. The inputs are directly communicated to the VA of the respective charger and are fundamental for the power-sharing among the VAs.

The CA has three main control functions - receiving measurements data, processing them and translating them into power setpoints according to the given control mode. The CA has three main control modes: constant mode, frequency regulation and RES mode. In constant mode the P_{CA}^{ref} is constant regardless of the conditions.

2.3.1 Frequency Regulation Mode:

In frequency regulation mode the CA receives frequency measurements from the PCC f_{meas}, and translate them in a power reference P_{CA}^{ref} according to the droop characteristic implemented which is generally defined as:

$$P_{CA}^{ref} = P_0 + k_{droop} \cdot (f_0 - f_{measured})$$

Figure 4 illustrates a simplified block diagram of the system working in frequency regulation mode. The power range, denoted as $P_{max} - P_{min}$, represents the amount of power the charging point operator allocates for frequency regulation. The power set-point corresponding to 50 Hz is defined as P_0. Provided that P_{max} and P_{min} are chosen within the power capacity of the PCC, they determine the controllable range of P_{CA}^{ref}. The droop control coefficient kdroop, is calculated as $\frac{P_{max} - P_{min}}{\Delta f}$. Each iteration of the CA ends with the broadcast of P_{CA}^{ref} to the VAs.

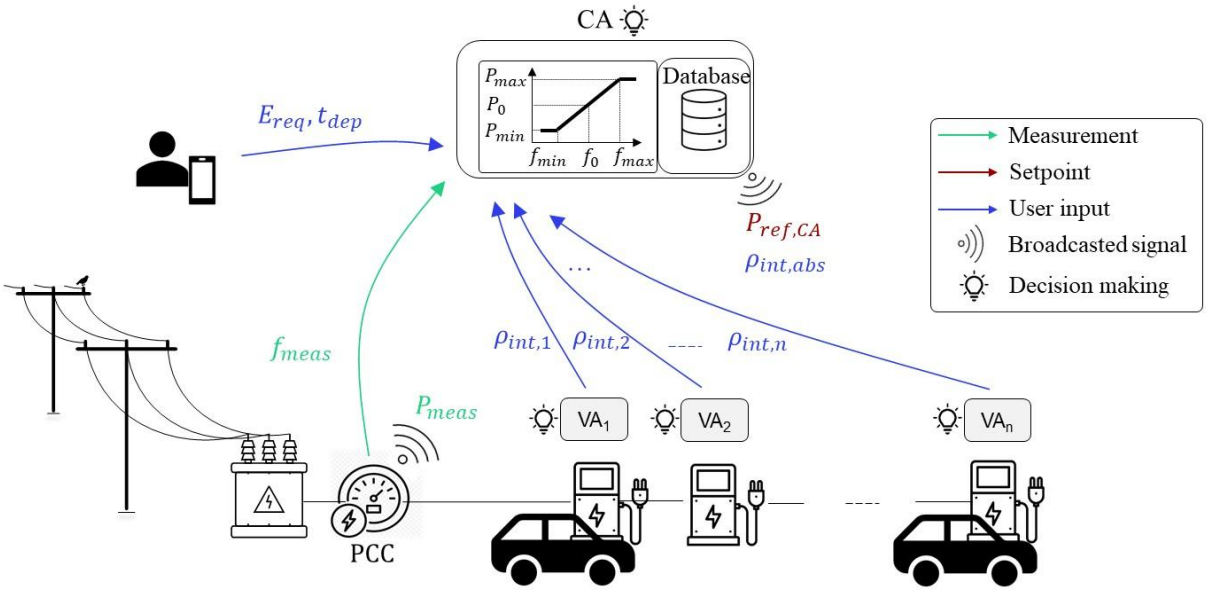

Figure 4: Simplified block diagram of the system performing frequency regulation.

2.3.2 RES mode:

On the other hand, the CA receives setpoints from the different RES devices such as PV systems and wind turbines in the RES mode, as shown in Figure 5Figure 5. The CA calculates P_{CA}^{ref} as:

$$\begin{cases} P_{CA}^{ref} = P_{PV} + P_{wind} + P_{import} \\ P_{cluster}^{min} > P_{CA}^{ref} \\ P_{CA}^{ref} \leq 43\ kW \end{cases}$$

Where P_{PV} is the total power produced by PV systems, P_{wind} is the total power produced by wind turbines and P_{import} is a control variable representing the power that the cluster is importing from the grid. Such control variable can be modified manually in the code. Another control variable that can be modified manually is $P_{cluster}^{min}$ which sets the minimum power setpoint that the CA can provide to

the cluster. $P_{cluster}^{min}$ is chosen to guarantee a minimum charging power to the EVs at all times. Finally, P_{CA}^{ref} cannot overshoot the connection capacity at the PCC, which for both clusters is 43 kW.

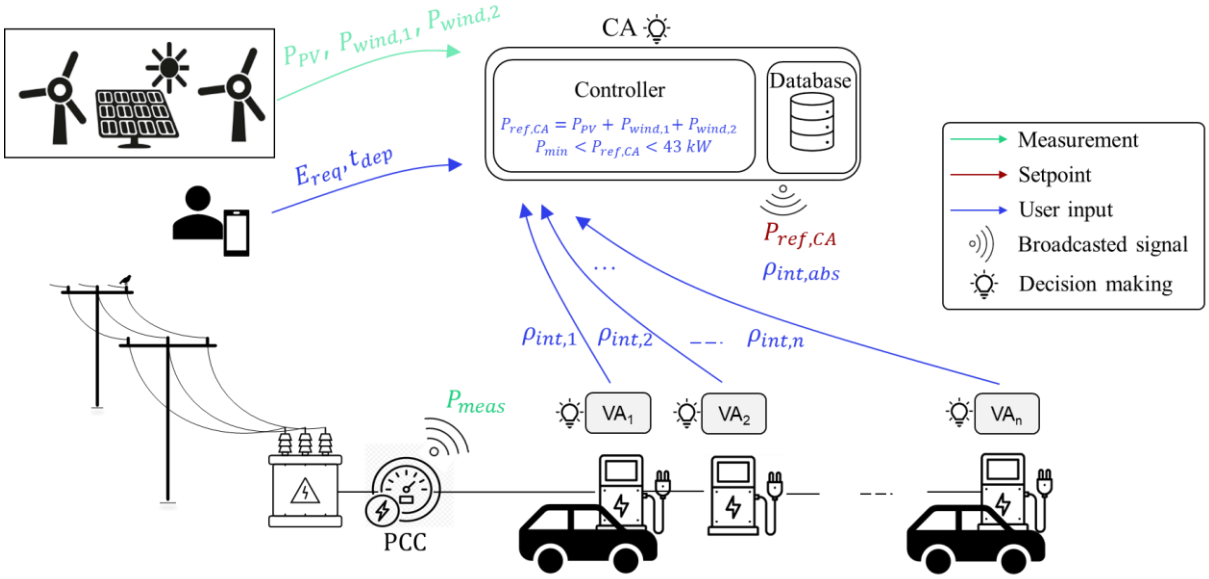

Figure 5: Simplified block diagram of the system performing RES following mode.

2.4 The Virtual Aggregator

The P_{CA}^{ref} is retrieved by the VAs together with the power measurement P_{meas} from the meter at the PCC. The two dimensions are going to be used to calculate the error as:

$$P_{error,PCC} = P_{CA}^{ref} - P_{meas}$$

There are two modes that the VAs can run with:

- The **normal mode** which consists of a priority-based algorithm for coordinating power sharing and power scheduling among the chargers.
- **Phase balancing** mode, which consists of an optimization algorithm for mitigating the unbalance levels on the three phases.

2.4.1 Normal mode

The VA residing in the chargers follows a logic referred to as the State Machine (illustrated in Figure 6), where each VA independently exhibits distinct behaviour and control actions based on its current state. The schematic figure outlines the states that each VA transitions through, determined by input data, local charger measurements, and predefined logic.

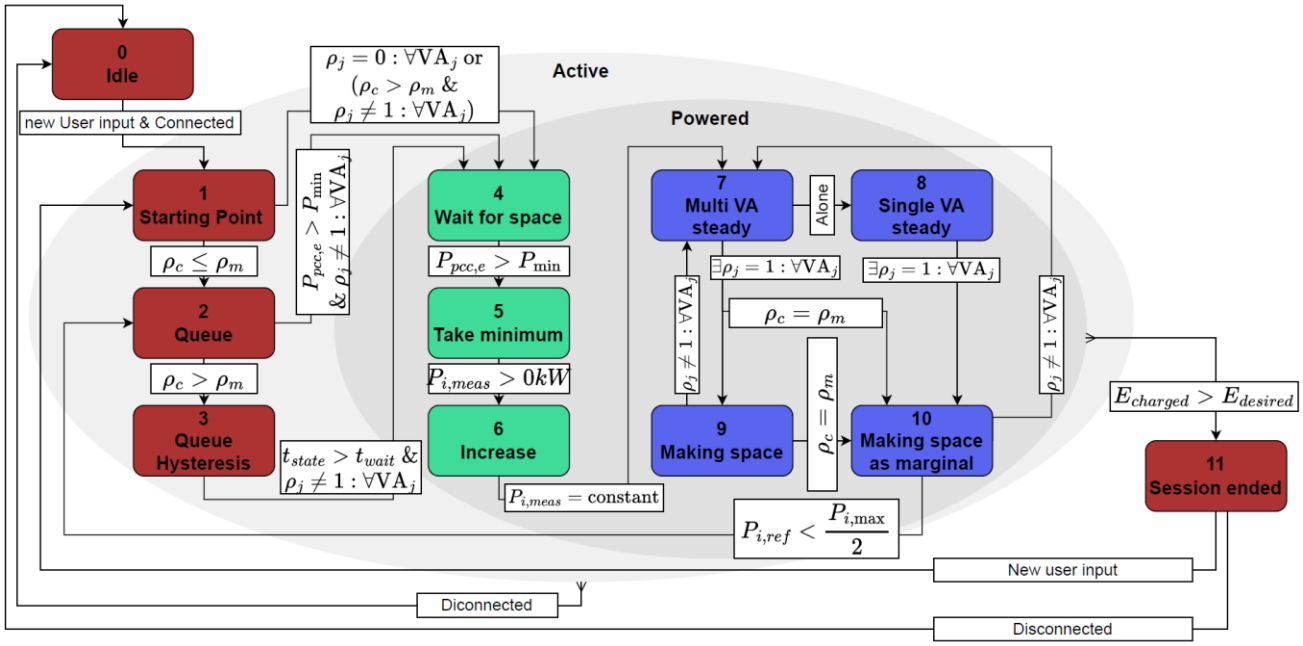

Figure 6: Flowchart of the State Machine describing every state and their conditions.

State 0 (Idle)

The idle state is the initial state, characterized by no connected EVs and an inactive VA. When a user connects and inputs the charging parameters, the VA transits to the Starting Point state. The user inputs are the requested energy E_{req} and the departure time t_{dep}. The inputs determine the internal priority ρ_{int} of each VA as:

$$\rho_{int} = \frac{E_{req} - E_{charged}}{(t_{dep} - t_0) \cdot P_{rated,EVSE}}$$

In the formula, $E_{charged}$ is the energy already delivered to the EV, measured by the plug during charging, t_0 is the current time, and $P_{rated,EVSE}$ is the rated power of the plug. The value of ρ_{int} ranges from 0 to 1 and serves multiple purposes: ρ_{int} is communicated among the chargers via the CA to indicate different states. A ρ_{int} value of 0 means that the VA is idle; a value going from 0 (not included) to 0.99 simply indicates the priority of the EV in any state; a value of 1 signals that the VA is initiating charging (states 4-6) and requires other VAs to adjust their consumption. Negative values indicate errors that require maintenance.

ρ_{int} is an intermediate step for the calculation of the relative priority ρ_r which is a key control parameter of the VA. Each VA calculates its relative priority ρ_r as:

$$\rho_r = \frac{\rho_{int}}{\sum_{i=1}^{N_{EVs}} \rho_{int,i}}$$

where $\sum_{i=1}^{N_{EVs}} \rho_{int,i}$ (denoted also as $\rho_{int,abs}$ in the figure) represents the summation of the internal priorities of all the chargers. While ρ_{int} is shared among the VAs, the ρ_r is not shared among the chargers.

State 1 (Starting Point)
At this point, the VA evaluates the cluster's conditions for entry. Entry is permitted if either the VA's priority ρ_{int}^{VA} is higher than or equal to that of the EV charging with the lowest priority ρ_{int}^{m} also called marginal charging session; ($\rho_{int}^{VA} \leq \rho_{int}^{m}$) while there is no other EV initiating the charging session (no VA is signaling ρ_{int} = 1), or there are no other EVs charging. If entry is permitted, transitions to initiation sequence (states 4-6), otherwise, the VA transitions to Queue (states 2-3).

State 2 (Queue)
In this state, the VA waits until cluster conditions allow entry. Two transition scenarios are possible: firstly, if the VA priority remains low, but sufficient power gap exists without requiring other VAs to make space ($P_{error,PCC} > P_{charger}^{min}$) , and no other VA is initiating, it transitions to initiation after a predefined interval ($t_{initialize}$). Secondly, if the VA priority surpasses the one of the lowest priority charging EV ($\rho_{int}^{VA} > \rho_{int}^{m}$), it moves to the Queue Hysteresis (state 3).

State 3 (Queue Hysteresis): The VA remains here for a predefined interval (t_{wait}). If no other VA begins charging during this period, it moves to the initiation sequence (states 4-6). This state prevents frequent rescheduling among EVs with marginal priority.

State 4 (Wait for Space)
As the first initiation state, the VA signals ρ_{int}^{VA} = 1, prompting the marginal VA to reduce power consumption while freezing the power consumption of the other VA charging. The VA waits until enough power margin ($P_{error,PCC} > P_{charger}^{min}$), is available before transitioning to state 5 (Take Minimum).

State 5 (Take Minimum)
Here, the VA initiates EV charging at the minimum power ($P_{charger}^{min}$). If the initiation fails, and the EV fails to start charging, the VA will go back to State 3 (Queue Hysteresis), in order to go back to State 4 (Wait for Space) after the predefined interval. Once the EV starts consuming the assigned power, the VA transitions to State 6 (Stabilize).

State 6 (Stabilize)
In this state, the VA keeps the power reference of the EV constant, and so do all the other VAs, having the system frozen for 15 seconds before all VAs go to State 7 (Multi VA Steady).

State 7 (Multi VA Steady)
State 7, is the state where the PI control for priority-based power sharing is happening. Each VA in this state will perform independently the calculation of the power reference for their charging session as:

$$P_{ref,i} = \begin{cases} P_{ref,i-1} + P_{error,PCC} \cdot \rho_r * k'_p & if\ P_{error,PCC} > 0 \\ P_{ref,i-1} + P_{error,PCC} \cdot (1 - \rho_r) * k'_p & if\ P_{error,PCC} < 0 \end{cases}$$

In the formula, *i* corresponds to the current iteration of the controller and *i*-1 to the previous iteration. The equations applied in two different scenarios based on the sign of $P_{error,PCC}$, outlines the operation of the PI controller. The proportional gain varies, being ρ_r when $P_{error,PCC} > 0$, and $(1 - \rho_r)$ when $P_{error,PCC} < 0$. This control approach ensures that EVs with higher priority will more readily increase their power demand in response to positive errors while reducing it less when the error is negative. In contrast, lower-priority EVs will have a smaller increase in power demand for positive errors and a larger decrease for negative errors. This strategy guarantees that EVs maintain their allocated share of power consumption dynamically, adapting to continuous changes in error, which may result from

fluctuations of the dynamic P_{CA}^{ref}. Moreover, $k_p^{'}$ represent an additional proportional gain, applied to all the VAs equally. This second proportional gain, represent the overall proportional gain of the control action of the EV cluster as a whole. Finally, each VA calculates its power reference $P_{ref,i}$ and communicates it to its charging plug. The control loop completes with feedback on $P_{meas,PCC}$ and P_{CA}^{ref} provided respectively by the meter at the PCC and the CA.

For each iteration the VA will check the conditions of the cluster from the different inputs it receives. For example, all other charging sessions are terminated (ρ_{int}= 0 for all other EVs), then the VA will switch to state 8 - Single VA Steady. On the other hand, if there is another EV in the initiation sequence (state 4-6), the VA will either switch to the state 9 (Making Space) or to state 10 (Making space as marginal), depending on its priority.

State 8 (Single VA Steady)
In this state the PI control is simpler, and it is defined as:

$$P_{ref,i} = P_{ref,i} - 1 + P_{error,PCC} * k'_p$$

Similarly to the previous state, if another EV is in the initiation state, the VA will transition to state 10 - Making Space as Marginal.

State 9 (Making Space)
In this state, the VA maintains constant power reference from the previous iteration ($P_{ref,i} = P_{ref,i-1}$), for the whole time an EV is in the initiation phase. After the EV is out of the initiation phase, the VA will return to state 7.

State 10 (Making Space as Marginal)
Triggered when another VA initiates charging and the current VA is marginal ($\rho_{int} = \rho_{int}^{m}$). The marginal VA reduces its power according to:

$$P_{ref,i} = P_{ref,i-1} + P_{error,PCC} - P_{charger}^{min}$$

This ensures a power margin of $P_{charger}^{min}$ maintained between P_{CA}^{ref} and P_{meas}.
If power drops below the minimum power ($P_{ref,i} < P_{charger}^{min}$) the VA will transition back to State 2 (Queue). Otherwise, after initiation concludes, it returns to state 7.

State 11 (Session Ended)
This state is reached either if the charging session is interrupted by the user or upon reaching user-defined energy requirement ($E_{desired}$).

2.4.2 Phase balancing mode

The proposed system introduces an optimal load management algorithm for public EV charging, designed to mitigate three-phase unbalance while operating under the limited available power in a charging cluster.
The algorithm is developed for heterogeneous fleets that include both single-phase and three-phase EVs, while ensuring compliance with phase unbalance constraints. A key feature of the system is a method for identifying the type of EV—whether single-phase or three-phase—allowing the smart controller to make appropriate load management decisions.

System Architecture
Each charger outlet is assumed to serve one EV at a time. A centralized smart controller dynamically manages the charging load of all connected EVs. The smart controller collects data from three main sources:

- **Users** – provide expected charging time and requested energy.
- **Cluster** – provides measured power on each phase and the electricity price, which reflects energy cost.
- **charger** – reports the measured charging power of the connected EV on each phase.

Information Flow and Decision-Making

- **Cluster Measurements**: These ensure that decisions are made within the system's operational limits, such as transformer fuse capacity or the output of local renewable energy generation.
- **Charger Measurements**: These enable the identification of the EV type. A single-phase EV only charges through one phase of the charger outlet, while a three-phase EV charges through all three. By checking whether any power flows on the second phase of the charger outlet, the controller can determine whether the EV is single- or three-phase. This information is then fed into the load management optimizer to allocate the correct charging power.
- **User Information**: Charging needs provided by users are incorporated into the optimization problem, ensuring that user demands are considered alongside technical constraints.

With these combined inputs, the smart controller formulates optimal charging decisions, dynamically allocating power while maintaining system balance.

2.5 Implementation of architecture

This subsection details the architecture implementation, including the hardware and software utilised. The VAs and the CA are hosted on "Beagle bone® black industrial" microcontrollers, which are equipped with an ARM Cortex-A8 1 GHz processor, 521 MB of RAM and 4GB of embedded flash memory. The microcontrollers are connected via Ethernet and deploy a Debian OS operating system. The control strategy is actuated on stand microcontrollers located outside the chargers, while the chargers are only responsible for the actuation of the final set-points. The chargers are linked to the Internet through a 4G connection, while all the other devices are connected to the university WiFi network, which is secured by a firewall. A public server database (Database 1 in the figure) mediates the communication through the firewall between the chargers and the microcontrollers. This server acts as a central hub and is the intermediate node of most control-related data communication.

The charging system incorporates an Android mobile app for providing user requests and monitoring the charging sessions. A web interface on the university server (Visualization Webpage) allows to monitor in real time the status of the cluster. The data management of the chargers is hosted on Amazon Web Services, which is responsible for the communication between the app, the chargers and the final power set-points from the VAs. The chargers convert the received power set-points to a current set-point, which is transmitted to the actuators. The charger follows the IEC 61851-1:2019 [90] type 2 charging protocol, using a 32 A 5-wire connection. Each charger has a total three-phase power capacity of 22 kW, distributed across two plugs, which are both capable of providing up to 22 kW of three-phase power. A smart meter (DEIF Multi-instrument MIC-2 MKII) at the PCC measures and publishes on the data broker energidata.dk (Database 2), different parameters on a second basis, useful for data storage and post-processing. All the data from smart meters of external devices, such

as transformers, RES and DEIF is handled with the framework of the Energy System Integration Lab – SYSLAB (Syslab node).

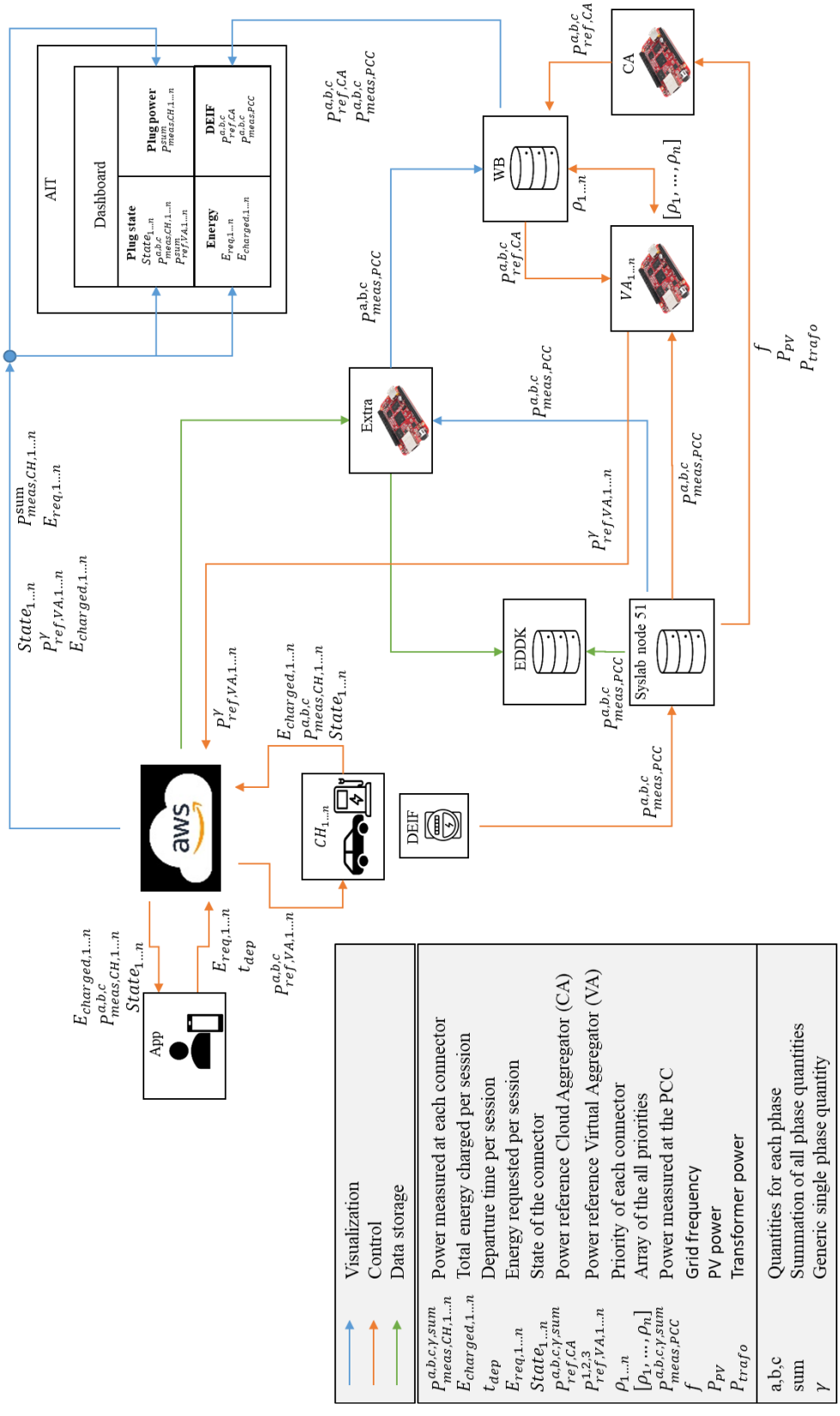

Figure 7: Complete block diagram of the architecture of the system.

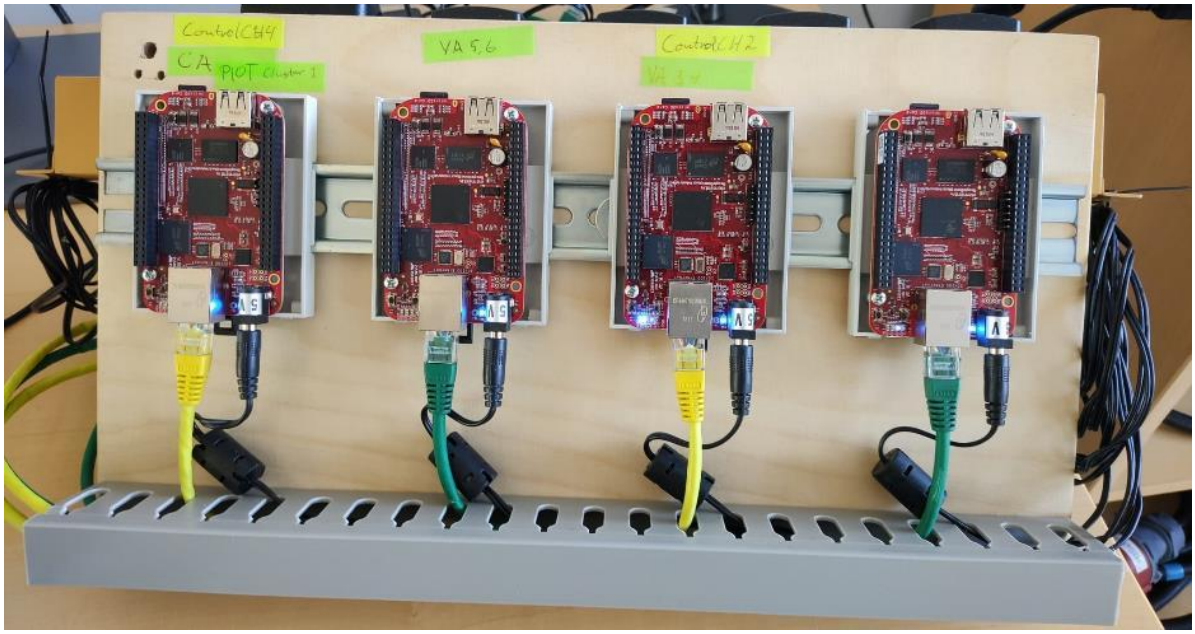

Figure 8: Beagle bones for the VAs of three chargers and the CA

3 Controllers validation in real conditions and lab demonstration

In the following paragraphs the experimental results of the different functionalities of the system are described. Most of the results were showcased during live demonstrations organized at the PowerLab laboratory in Risø.

3.1 Transformer Protection

A demonstration of the capability of the architecture to adjust its charging power in order to avoid transformer overloading is presented in Figure 9: .

The transformer loading limit is set to 10 kW. At 2100s RES production was shut down and thus we see no more power export (no negative values of P_{Trafo}) in Figure 9: . The LEAF1 is connected and started to charge at around 2200 s. At 2300 s LEAF2 is connected and since the chargers consider the EVs to charge with three phases, the first LEAF leaves space for the second diminishing the charging power. Then, they both are charging at 5 kW – sharing power and without exceeding the established transformer limit.

At 2370 s an external controllable load of 40 kW is connected. The transformer has a power import spike of 50 kW. After a few seconds, the TRAFO protection mode was deployed: the EVs reacted to the transformer overloading and stopped charging to mitigate the power congestion (shown in purple circles in the figure.

At 2410 s the external load is disconnected, thus relieving congestion of the transformer and, with an 8 s delay, the EVs started to charge again, reaching the transformer limit.

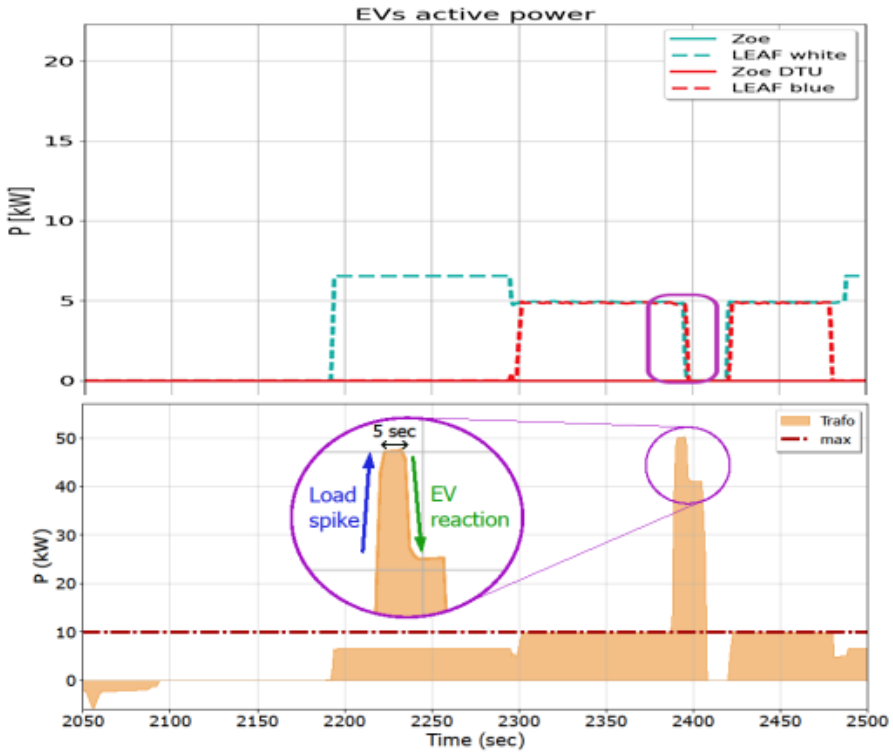

Figure 9: Active power of EVs (top plot) and at transformer (bottom plot) in the TRAFO

3.2 Frequency regulation mode

In a Figure 10 time history of the frequency regulation performance is provided. The test is provided using one charger to which two Renault ZOEs are connected. In the above graph there is an overview of 1 hour ca. of frequency regulation. In both graphs the blue line represents the frequency time history, the red line represents the power utilized by the cluster. The power adjustment is performed equally by the two EVs, as equal priority was given to them. During the test a power bid of 6 kW is provided to a hypothetical flexibility market. The droop control has a base value of 15 kW at 50 Hz frequency and offers $\pm$ 3 kW for the frequency range 50.1-49.9 Hz. The top graph shows correct and robust performances. On the other hand, the bottom graph illustrates a smaller portion of the same test, to focus on the delay of the chargers in following the frequency. The graph shows a delay ranging from 15 s to 11 s roughly. The delay depends on different factors currently under analysis: together with the delays in communication and actuation of the control signals, an important factor is the reaction time of the cars, which is different for every brand and model.

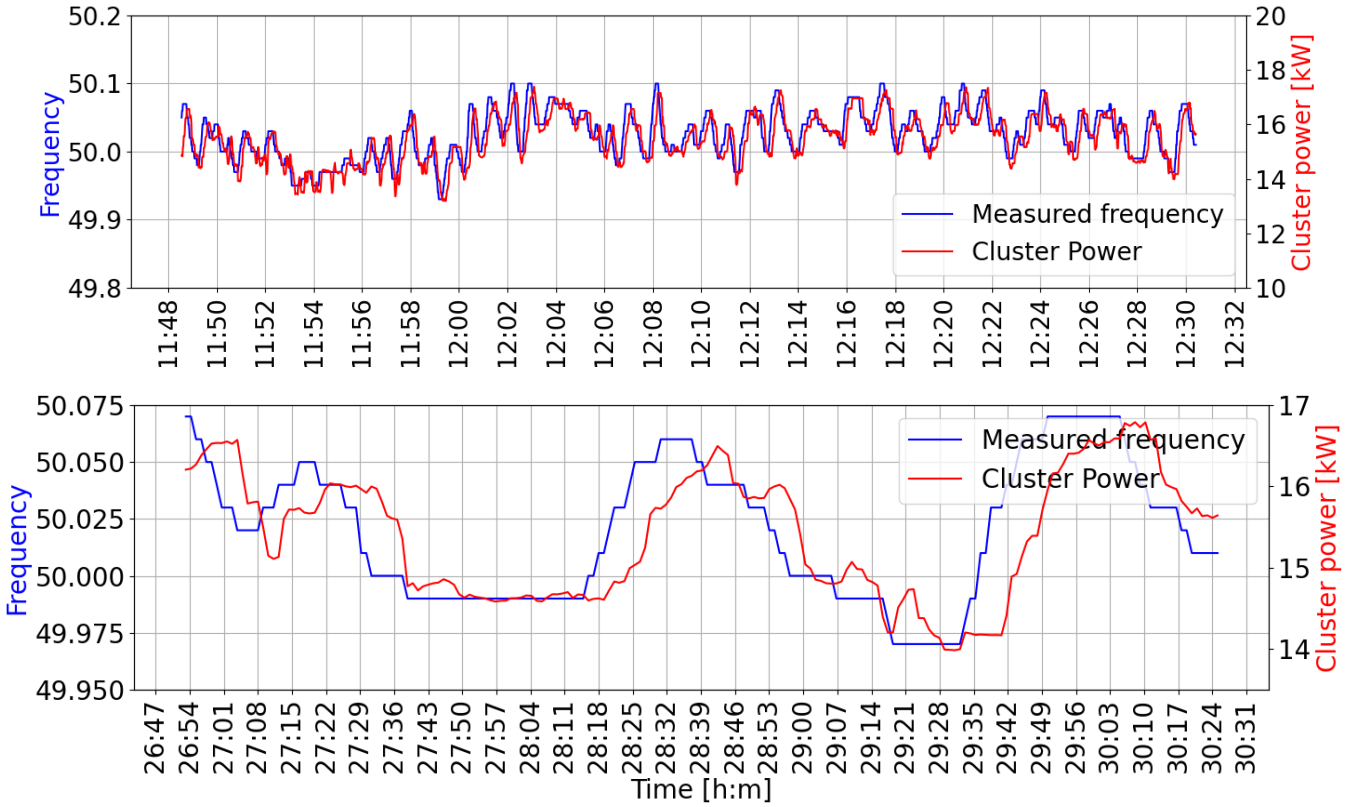

Figure 10: Frequency regulation time history. The graph below is a zoomed instance of the above graph for better time visualization. The blue lines illustrate the frequency while the red lines illustrate the Power utilized by the cluster.

Figure 11 and Figure 12 respectively show the development of the EVs' priority over the testing period and the power consumption of each individual EV. During the test, equal priority was given to both EVs. The priority graph shows that the difference between the two cars is neglectable. However, from during the end of the test, EV2 shows a decrease in power consumption, leading to a slower decrease in priority. This behavior, although marginal, could be explained by many factors. The most reasonable hypothesis is that EV2 might be slightly undershooting the power allowed by the chargers due to internal reason (e.g. higher SOC, different temperature etc.).

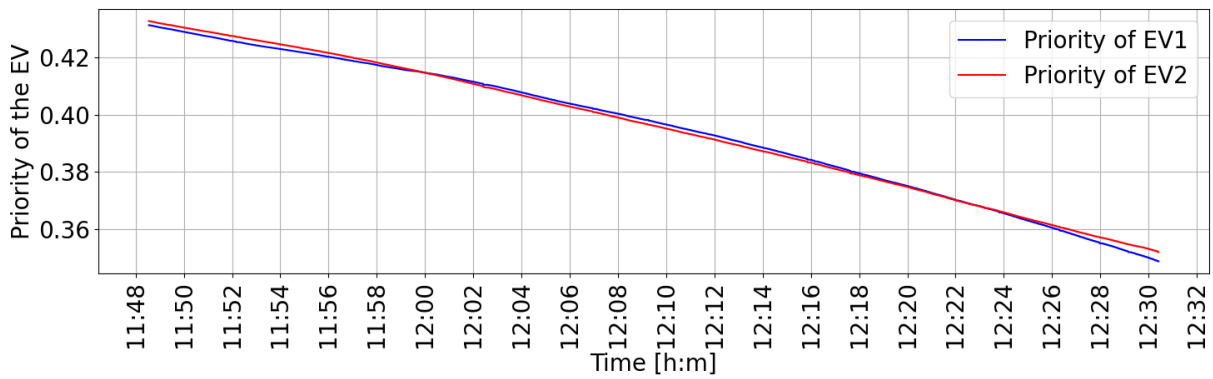

Figure 11: Time history of the priority of the two EVs during the frequency test.

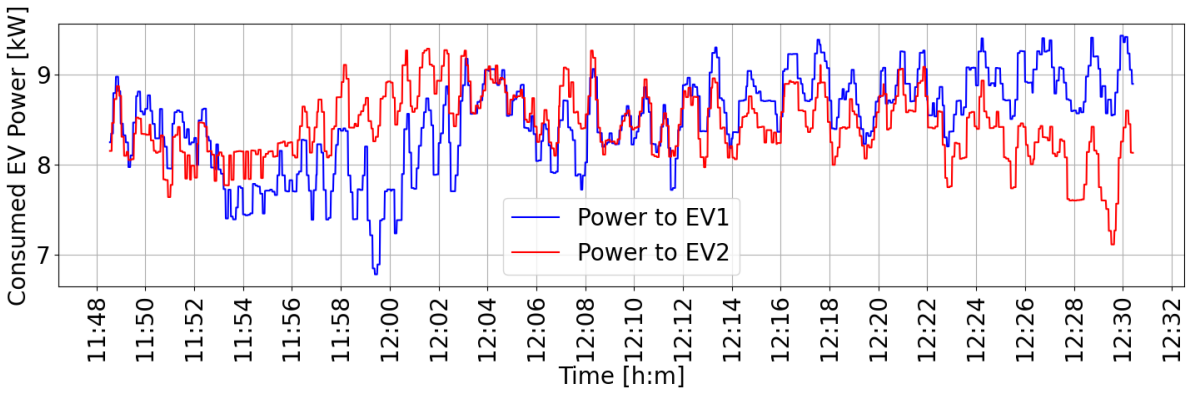

Figure 12: time history of the individual EV power consumption

3.3 Scheduling and priority

The last functionality demonstrated in the project is the capability of the developed chargers to schedule the charge between two different EVs according to the users' inputs. During the test, two cars with very similar energy request and departure time are connected to the chargers. For the scope of the demonstration the scheduling interval in the VA control is reduced to 0 s: this means that the chargers would alternate the charging to each EV as long as the priority is just marginally different. As shown in Figure 13, the resulting time window for each EV is therefore just a few minutes, giving the possibility to show 3 scheduling events in a small period of time. It is important to clarify that a charging power value of 0 kW in the results does not represent a below-minimum charging current signal is being delivered to the EV. Instead, when an EV's priority decreases and its charging session is temporarily paused, the charger transitions the control pilot signal from State C ("charging") to State B ("connected") in accordance with IEC 61851. In this state, no charging current is commanded, while the physical connection remains intact. When charging resumes, the charger returns to State C and applies a PWM duty cycle corresponding to a current equal to or greater than the minimum charging lever.

Figure 14 illustrates the change in priority between the two EVs charging. In the graph, the first EVs starts charging: while the charging schedule is starting, the priority is 1 (the maximum priority value). When the EVs power reaches a steady state (as shown in Figure 13) the priority is then reduced to the priority value corresponding to the urgency of the charging session. As previously mentioned, the urgency of the charging session depends on the energy requested and by the time of departure stated by the user in our website. The visualized priority of the other EV is 0 for clarity purpose, although the real priority is memorized in the charger. The priority of the charging EV is slowly decreasing as energy is accumulated. When the priority of the charging EV becomes lower than the priority of the other connected EV, the schedule of the second EV takes place. Therefore, the first EV stops charging, and its priority becomes 0. On the other hand, the second EV starts charging and its priority becomes 1. The cycle then continues until both charging fulfilment is reached.

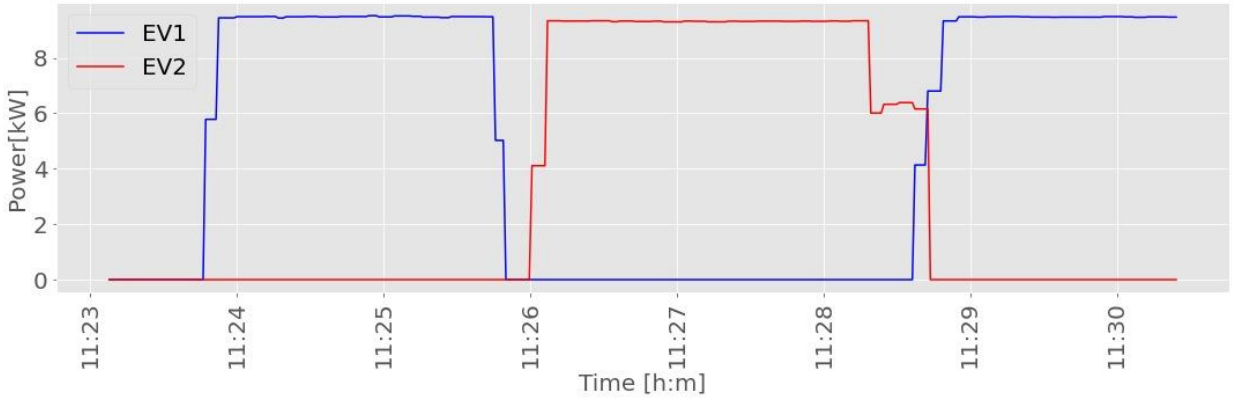

Figure 13: Power scheduling between two EVs.

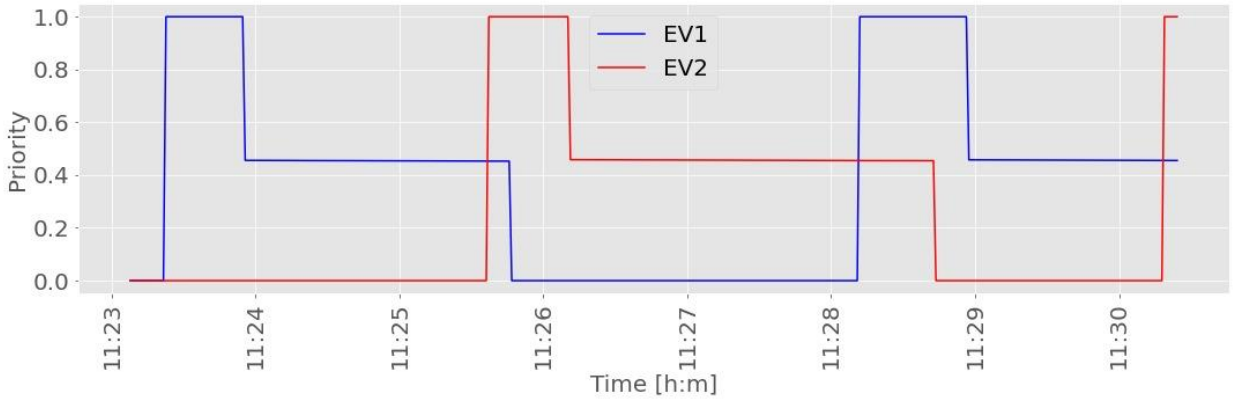

Figure 14: Priority trend during the power scheduling test.

3.4 RES following mode

A demonstration of the RES following mode was conducted through a three-and-a-half-day test at the Risø parking lot, which is a real implementation of our charging setup. During this test, no restrictions were placed on the types of EVs or the timing of their arrivals. Instead, people from the department and nearby offices were invited to freely connect their vehicles, allowing for natural and uncontrolled charging behavior.

The renewable energy used in this experiment was supplied by two PV systems installed on top of Building 330 in Risø, each with a rated power of 20 kW, as well as by two wind turbines: the Gaia turbine with a rated power of 12 kW and the Aircon turbine with a rated power of 10 kW. To guarantee a minimum level of service, the system was configured with a lower threshold of approximately 2 kW. Whenever renewable generation dropped below this threshold, the deficit was covered by importing energy from the parking lot's grid connection.

Figure 15 showcase the time history of the experiment. The graph illustrates the power production from renewables (in grey) and the power consumption (in blue, green and red) across the three phases. In several instances, the consumption lines for each phase do not perfectly overlap. This is explained by the presence of single-phase EVs, which naturally cause minor phase unbalances. Despite this, the

overall results confirm that the system is capable of effectively following the renewable generation profile, particularly when enough EVs are connected and charging.

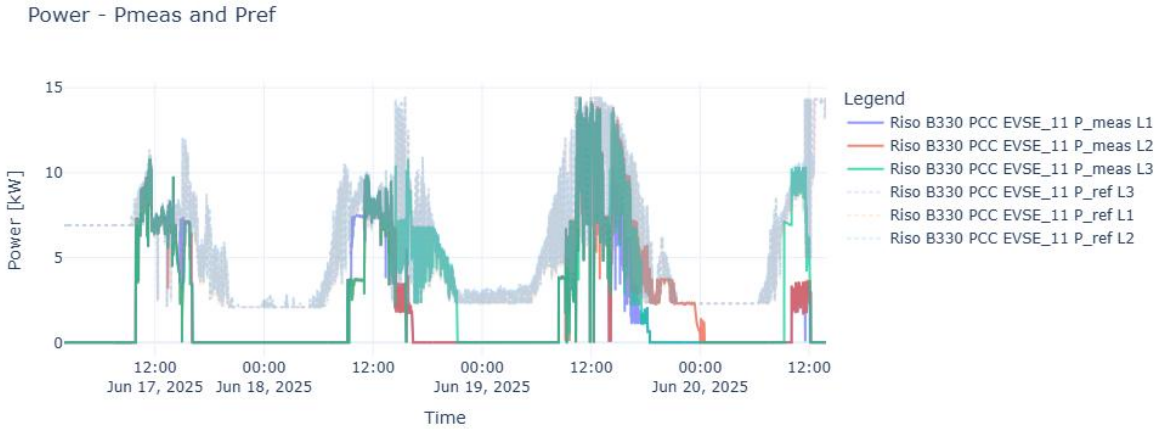

Figure 15: Power consumption and power measurement at the PCC for the parking lot during RES following mode

3.5 Phase balancing mode

The proposed algorithm was validated through experimental case studies conducted on the Riso campus, designed to replicate realistic EV user charging behaviors. The experiments were carried out in **renewable charging mode**, where the available charging power for the cluster was supplied exclusively by local photovoltaic (PV) and wind generation. In this mode, the total charging power for the cluster could not exceed the renewable supply on any phase.

Experimental Setup

The experiment took place on 18th March 2025 at the Riso campus, involving three EVs connected to charger outlet 1321, 1322, and 7541. Among them, the EV at plug 1321 was a single-phase vehicle, configured to charge on phase B of the parking lot, while the EV at plug 1322 was a three-phase vehicle.

The charging infrastructure operated under defined power constraints. The maximum current allowed for each charger outlet was set at 16 A, corresponding to 3.68 kW, while the minimum allowable current was 7 A, equivalent to 1.61 kW. To ensure system stability, the phase unbalance limit was set at 10 A, or 2.3 kW. This meant that at all times the smart controller regulated the charging process so that the difference in power between any two phases did not exceed 2.3 kW.

Figure 16: time series of the experiment. The top three graphs show the power consumption over time for each EV while the bottom three graph show the power reference from CA.

Observations

1. **Initial Charging (EV 1322 only)**
    - EV 1322, a three-phase EV, connected first.
    - With sufficient renewable supply, it charged at full power, drawing equal current across all three phases and maintaining complete phase balance.
2. **Second EV Connection (EV 1321 added)**
    - When EV 1321, the single-phase EV, connected on phase B, the power demand on that phase increased.
    - Renewable power on phase B was insufficient to supply both EVs at full capacity.
    - Since EV 1322 distributes charging evenly across all three phases, the unbalance was caused entirely by EV 1321.
    - To maintain the unbalance limit, the controller restricted EV 1321 to 2.3 kW, while allocating the remaining power on phase B to EV 1322.
    - Consequently, the charging power of EV 1322 adjusted dynamically to follow the available renewable generation.
    - Because EV 1322 must charge equally on all three phases, its power on phases A and C was also reduced, resulting in a parallel reduction across all phases.

3. **Disconnection of EV 1322**
    - When EV 1322 disconnected, only EV 1321 remained active.
    - Its charging power was fixed at 2.3 kW on phase B, as dictated by the unbalance constraint.
4. **Re-connection of EV 1322**
    - EV 1322 later reconnected. However, due to its high state of charge (SOC), its charging power gradually decreased, eventually falling below the minimum charging threshold (1.61 kW per phase).

Outcomes

The experiment demonstrated that the controller effectively maintained system stability and respected user requirements, renewable supply limits, and phase unbalance constraints. In all scenarios, the algorithm dynamically adjusted charging allocations to optimize resource use while keeping phase differences within the set 2.3 kW limit.

Conclusion: The proposed system successfully managed EV charging in a real-world setup, proving its capability to balance user demands, renewable energy availability, and technical limitations.

4 Key Performance Indicators (KPIs)

The following chapter describes the high-level performance and utilization of the parking lot and the KPIs for the deployment of the smart charging infrastructure as part of the EV4EU deliverable. The KPIs are divided in Technical KPIs, Economic KPIs, users KPIs and Environmental KPIs.

4.1 Technical KPIs

Uptime of chargers

In order to understand the chronological aspects of the operation it is important to understand the timing of the installation of the chargers on the campuses and the offline time of the whole parking lot. During the period of analysis, not all the chargers were present on the two campuses and some chargers were sent back and forth to the partner company - Circle Consult, prototyping them for updating or maintenance.

As more chargers become installed, operational, and begin logging data in the energydata.dk database, the number of recorded entries is decreasing, and the system requires more time to transmit data from the growing charger group to the database.

The system also shows some periods where the whole cluster is offline, this is due to the whole Syslab system being offline for maintenance or some problem external to the charging system and infrastructure.

The analyzed time of operation spans from 01-11-2024 to 31-12-2025 which is the time of full completion of the data logging system.

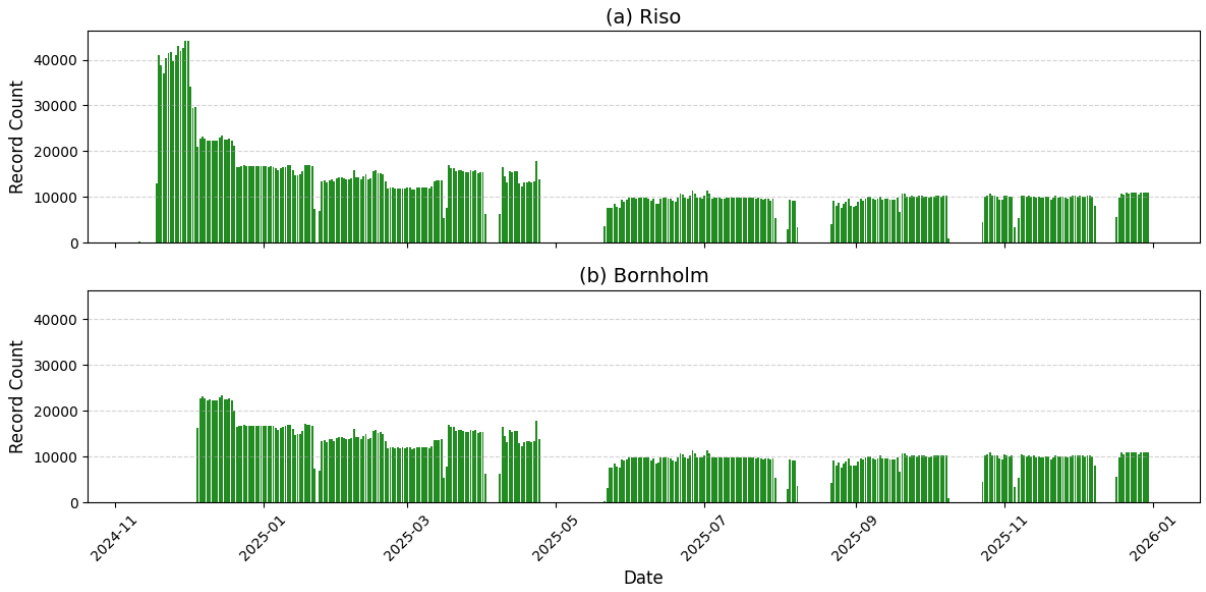

Figure 17: Recording charging entries in Risø and Bornholm parking lots

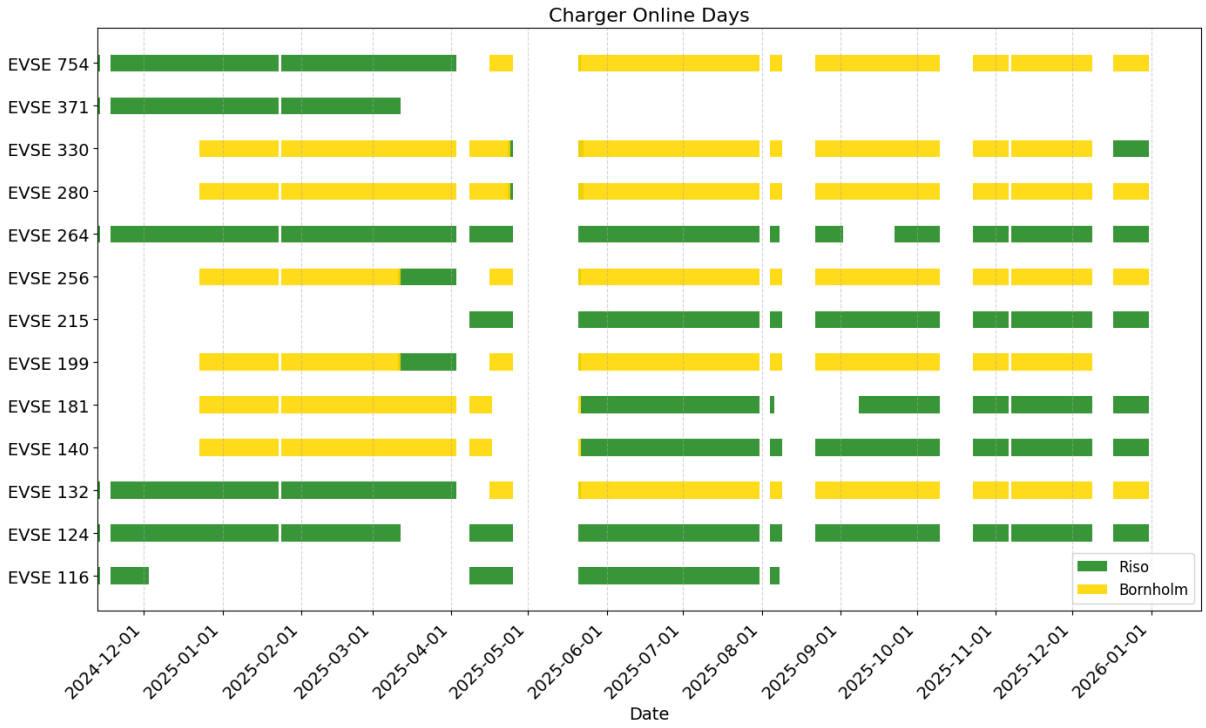

Figure 18: Online period of the chargers in Risø and Bornholm parking lots

Figure 18 shows the online period of each charger, to provide an assessment of the installation and operation of the chargers at the Risø parking lot over the period under analysis. From the graph it is possible to see when the chargers have been dismounted for maintenance and therefore went offline.

Total capacity

The total capacity at the PCC for each parking lot is 43 kW three phase connection, meaning 14.4 kW per phase, 63 A per phase. At the final stage of the implementation, both parking lots have now 6 chargers each, each with a power capacity of 22 kW to be shared among the two plugs of the charger. Each plug can maximum consume 22 kW.

Power Factor

The power factor, gives an estimate of the general behaviour of the parking lot and the possible effects of the power modulation of the EVs on the reactive power consumption or production of the parking lot as a whole. Different EV models have different power factors characteristics as they are modulating their power from the rated power to the minimum charging power. Generally, the lower the charging power of an EV, the more the power factor deteriorates. One expected trend would be that as the amount of charging EVs increases, each EV would modulate their power consumption in order not to overshoot the connection capacity at the PCC and therefore the power factor is supposed to decrease. The figure below, shows the average power consumption at the PCC, regardless of the number of EVs connected in relation to the average power factor. Although the two trends don't show any visible proportionality, the average power factor shows a general downward trend throughout the day, which possibly indicates an increase of the power factor as the EVs reach full charge.

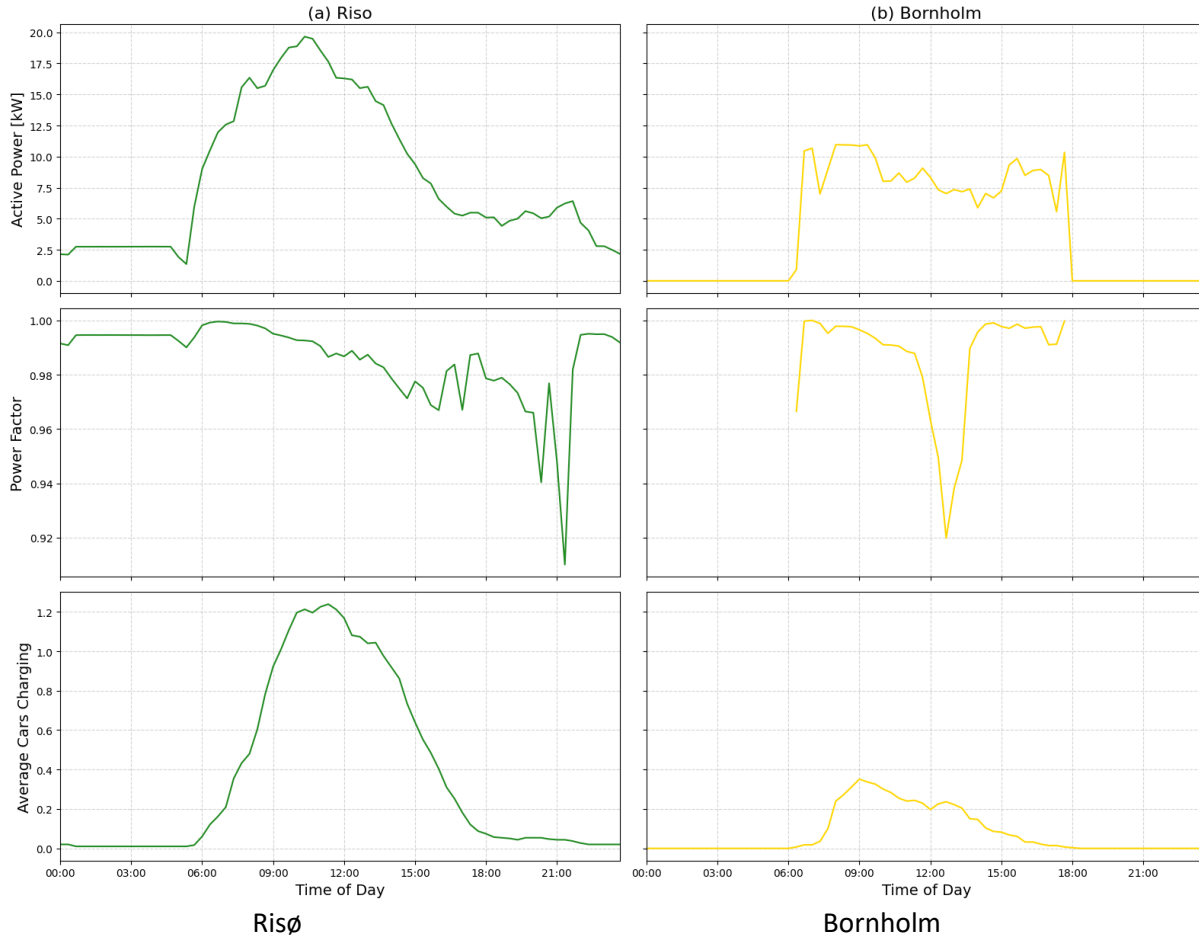

Figure 19: Average active power, power factor and number of EVs charging in Risø and Bornholm parking lots

Potential flexibility

The potential flexibility is calculated according to the methods presented below. The developed method assesses the flexibility of a parking lot in three different domains: namely power, time and energy. The method provides the following flexibility indexes:

Minimum Power Flexibility Index (MPFI):

$$MPFI = 1 - \frac{P_{max,avg}}{CC}$$

Measures the remaining power flexibility during peak demand by comparing the average maximum charging power $P_{max,avg}$ to the grid connection capacity CC. A higher MPFI indicates more available power flexibility when the system is most loaded.

Average Power Flexibility Index (APFI):

$$APFI = 1 - \frac{P_{mean,ch}}{CC}$$

Assesses the average power flexibility during charging periods by comparing the average charging power dispatched $P_{mean,ch}$ to the connection capacity CC. It reflects how much the charging cluster can adjust power under typical conditions.

Energy Flexibility Index (EFI):

$$EFI = 1 - \frac{E_{ch}}{E_{pot}}$$

Indicates the cluster's ability to delay energy delivery by comparing the actual energy delivered $E_{ch}$to the potential energy demand E_{pot}, where a higher EFI means more flexibility in shifting energy consumption over time.

Time Flexibility Index (TFI):

$$TFI = \frac{t_{tidle,avg}}{t_{tot,avg}}$$

Quantifies how much charging sessions can be shifted without affecting total energy delivery, by measuring the ratio of average idle time when fully charged $t_{tidle,avg}$ to the average total connection time $t_{tot,avg}$.

For more details on the methodology the reader is referred to the reference paper "Flexibility potential quantification of electric vehicle charging clusters".

The scores on these indexes over the analyzed period for the Risø and Bornholm parking lot are illustrated in Figure 20. For Risø campus, the MPFI is 0.49, showing that on average the power consumption during peak utilization is 49% of the connection capacity. The APFI is instead 0.69, which further confirms the low power utilization of the parking lot on average. The EFI of 0.52 shows that also on the energy domain there is flexibility, with the parking lot capable of providing 52% more energy, without compromising charging fulfillment. On the other hand, the TFI is relatively low, showing that the EVs on average spend only 26% of the connection time in idle mode. One of the possible reasons why such TFI value is that the power capacity of the plugs is limited to 11 kW, lengthening the charging time of the EVs. Moreover, limiting the charging power to 11 kW would lower the charging efficiency and degrade the power factor for most EVs, increasing losses and further slowing down the charging sessions.
Compared with Risø parking lot, Bornholm parking lot delivers similar performance but with even higher flexibility, the reason attributes to the fact that Risø parking lot was busier with more user coming for charging.

Overall, the flexibility indices show that the parking lot has high flexibility potential in all domains, and that the time of connection of the EVs is enough for full charging fulfillment of the charging sessions.

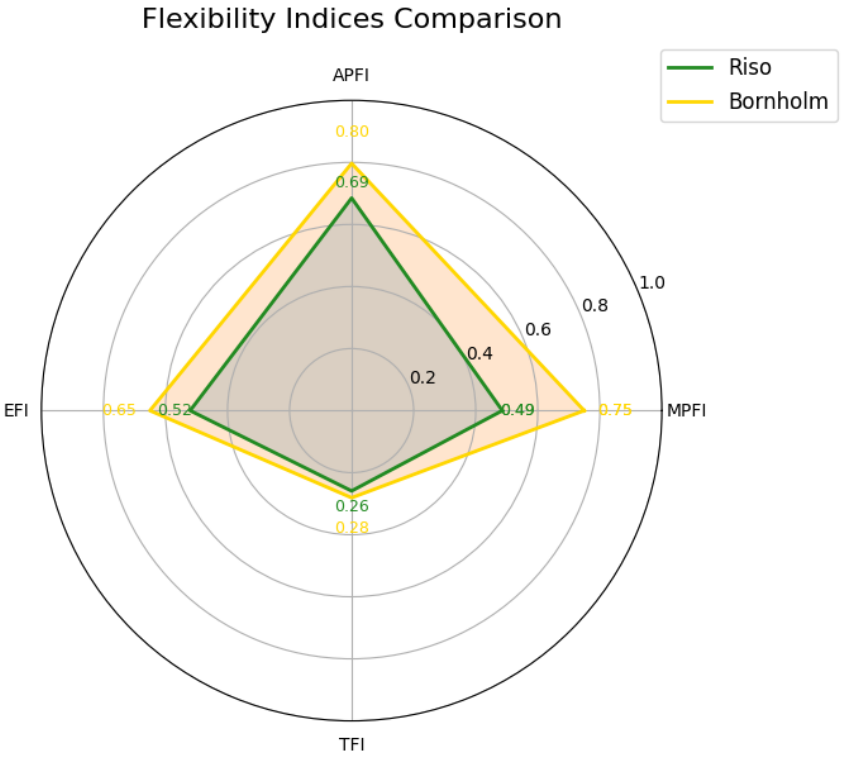

Figure 20: Flexibility indices of Risø and Bornholm parking lot

Requested flexibility

Although in this project there haven't been developments regarding flexibility services or external requests from grid operator, we could provide an estimation of the requested flexibility that the parking lot could provide as a function of the potential flexibility, also taking into account the average amount of energy that the parking lot could provide.

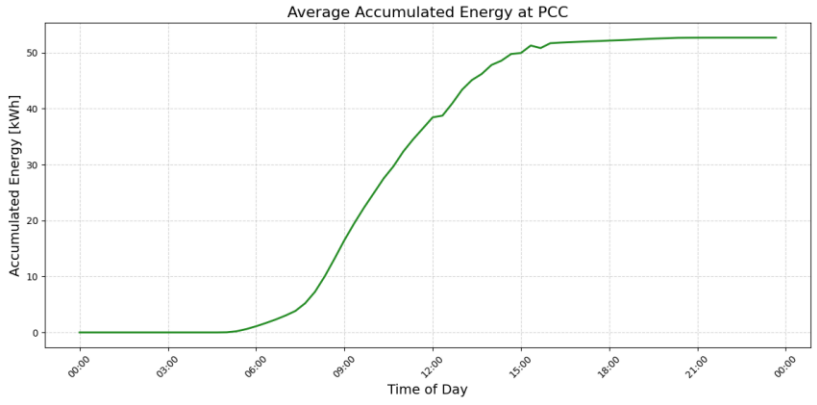

Figure 21: Daily average energy accumulated in the EVs

Figure 21 describes that the daily average energy accumulated in the EVs is roughly 50 kWh over the analysed period.

Charging success ratio (CSR)

This KPI estimates how effective the average fulfillment of the charging sessions with a value between 0 and 1. The formula of the CSR for each charging session is defined as:

$$CSR = \frac{Energy\ delivered}{Energy\ requested}$$

The CSR is therefore defined as a ratio between the energy delivered for the charging session and the energy requested by the user. One of the problems related to the estimation of energy requested is that the mobile app for user inputs was still under development during the analyzed time. Therefore, the chargers were mostly utilized by the technical personnel and often for testing, the inputs were given directly via computer software used for development. Hence the user inputs in this analysis are going to be disregarded as they are not representative of real user behavior and request. In replacement of the real energy request, we are going to calculate a virtual energy request from the user, which is equal to 9 kWh per hour of charging time. 9 kWh is roughly the maximum energy that an average EV can charge in an hour if it receives a setpoint of 11 kW. Because of the power factor degradation and precision of the controller, most cars receiving a power setpoint of 11 kW will only charge to roughly 9 kW.

This approximation, although generally true, leads to some minor underestimations and overestimations that we consider acceptable for the scope of the report.

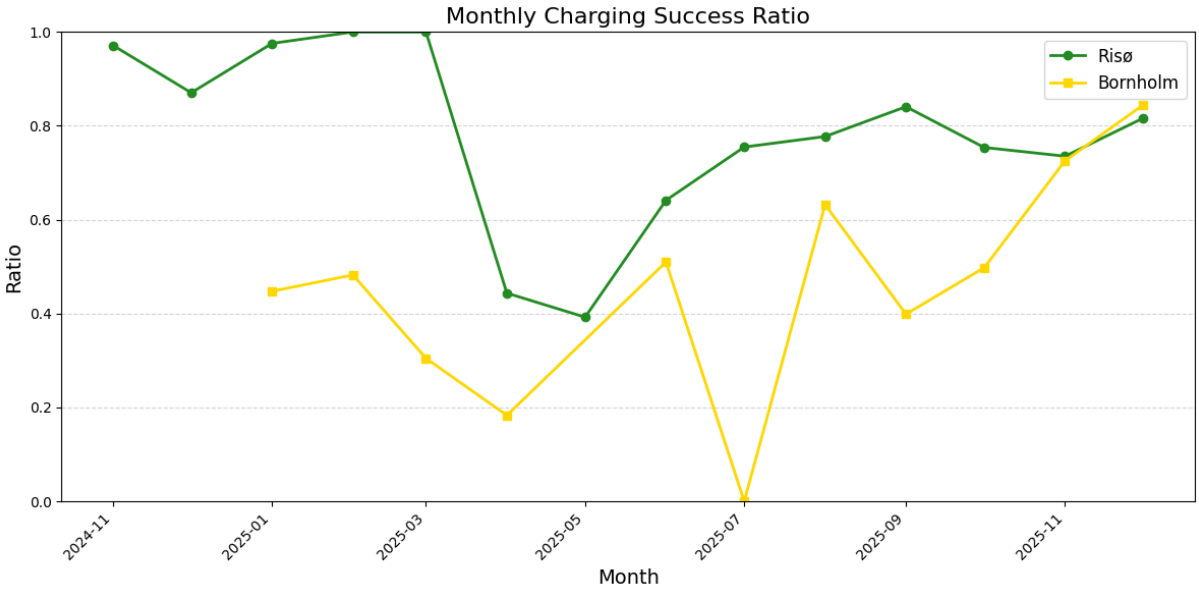

Figure 22: Monthly average charging success ratio in Risø and Bornholm parking lots

Figure 22 shows the monthly average CSR for all the charging sessions over time. Overall, we can see that the CSR oscillates from 0.5 to 1.0 for Risø and 0.2 to 0.8 for Bornholm.

Setpoint compliance

This KPI concerns the precision of the cluster of chargers in following the power setpoints provided by the central controller of the parking lot. In this KPI we measured the delay and accuracy of the chargers in following a setpoint precisely. The measurements are performed in the laboratory by using cross-correlation to compare the time difference at the PCC between the detection of a triggering event and the full response of the parking lot.

The normalized cross-correlation peaks at 0.98 at a lag value of 8.48 seconds. Such a result, although semi-quantitative, tells us that the two curves have a very high degree of similarity, but the measured power curve is delayed by 8.48 seconds compared with the expected power curve. The delay is caused by different factors: together with the delays in communication and actuation of the control signals, along with an important factor of the reaction time of the EVs.

Finally, the right subplot illustrates a histogram of the error distribution between the measured power and the expected power during the test. For this analysis, the measured power was shifted by approximately 8.48 seconds to highlight the controller's precision and minimize the influence of the controller's delay on the calculation. Additionally, the error ranges from -1.08 kW to 0.48 kW. The 98% percentile range of error values lies between -0.73 kW and 0.29 kW, indicating that the probability of an error greater than 0.29 kW or less than -0.73 kW is 1 % in both cases.

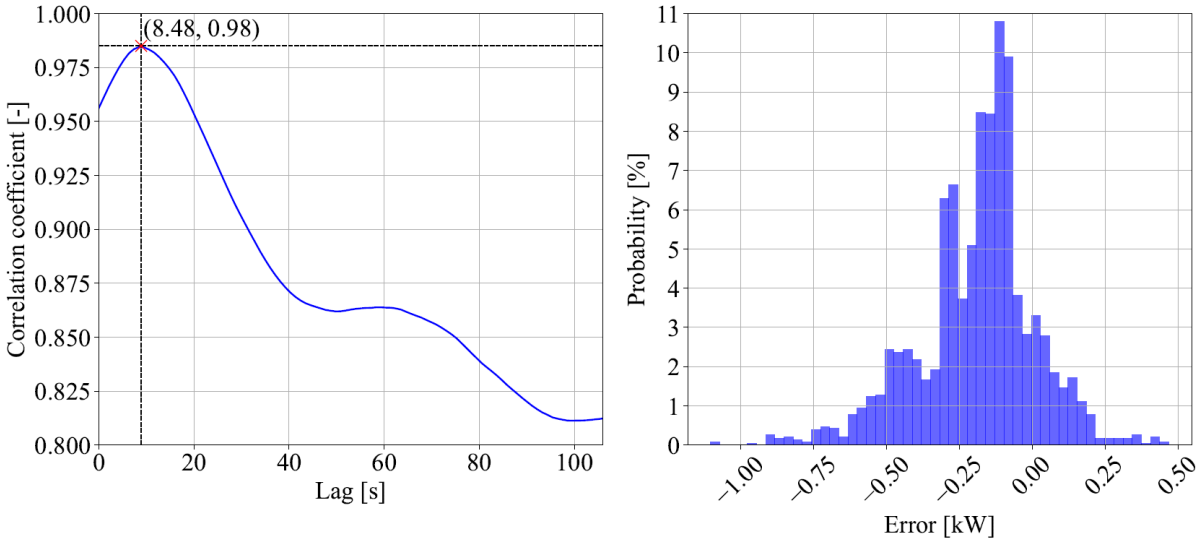

Figure 23: Time delays and the correlation at the PCC between the detection of a triggering event and the full response of the parking lot.

4.2 Economic KPIs

KPI_DK_2 Cost of provided energy

This KPI is related to the cost of provided energy for the charging point operator (DTU) during the analyzed time of operation. The data is calculated based on the consumption measured at the PCC and the hourly electricity price found in the Nordpool datasets. Figure 24 shows a bar graph with two bars for each month: in green the cost of energy without accounting for the self-consumption from the distributed renewable energy sources available for the workplace building, while in yellow the reduced price after taking into account the self-consumption and therefore the reduced energy import from the grid.

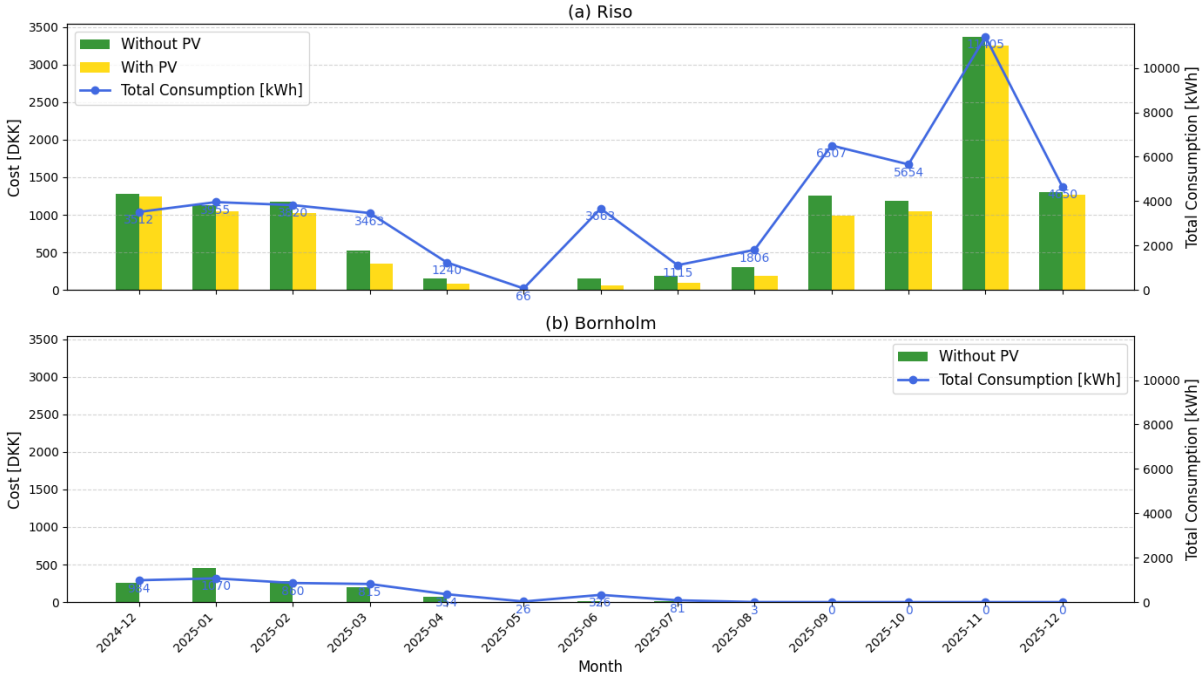

Figure 24: Cost of energy with and without accounting for the self-consumption from PV in Risø and Bornholm parking lots.

Figure 24 illustrates an overall reduction in the price paid going from December 2024 to December 2025 in both cases. In May there is no price at all, and in July it is increasing again. This trend, overall cannot be generalized to other workplace parking lots, because there are factors that were affecting it:

1. During the period under analysis, the development of the hardware and the user application for Android and IOS phones is still ongoing, and therefore the chargers were undergoing frequent updates, which increased the downtime of the parking lot in general.
2. The downtime of the system and the coming of the warmer weather might have driven down the number of users coming to the parking lot, especially in May, during which the Danish Cyclists' Federation runs an annual campaign called "Bike to Work" (Vi Cycler Til Arbejder). This campaign is a competition going on during the whole month of May, where different workplaces create a team and compete on the number of days and kilometers are cycled to work.

On the other hand, the contribution from local renewable energy sources can also be observed in warmer season that the gap of the cost between with and without PV scenarios in Risø parking lot is greater than the counterpart in colder weather due to the increase of solar energy.

KPI_DK_4 Self-consumption and self sufficiency

The table below illustrates the results for self-consumption and self-sufficiency for the parking lot system during the analysed time. The two KPIs are calculated as:

$$\text{Self consumption} = \frac{Energy\ consumed\ by\ EVs\ from\ PV}{Total\ PV\ energy\ produced} * 100$$

$$\text{Self sufficiency} = \frac{Energy\ consumed\ by\ EVs\ from\ PV}{Total\ EV\ energy\ demand} * 100$$

The table illustrates that the self-sufficiency is generally higher than the self-consumption in warm seasons and lower in cold seasons. During the whole period, the EVs utilize at least 4% of the energy produced by the PV for charging. The self-sufficiency peaks in May, where all the energy consumed (which is almost zero as described in the previous section) comes from PV.

On the other hand, self-consumption has a reversed distribution compared with self-sufficiency. This is because PV could only provide limited energy during the cold seasons, hence it exported less to the grid. The trend has a maximum in November, where the rate is 61%, and a minimum in March, where the self-consumption so low to be rounded to 0%, because most of the power from the RES is exported into the grid.

Month	Self Consumption [%]	Self Sufficiency [%]
2024-11	56.0	7.0
2024-12	35.0	7.0
2025-01	43.0	13.0
2025-02	38.0	27.0
2025-03	0.0	54.0
2025-04	15.0	63.0
2025-05	2.0	100.0
2025-06	16.0	65.0
2025-07	8.0	61.0
2025-08	21.0	43.0
2025-09	37.0	40.0
2025-10	58.0	21.0
2025-11	61.0	5.0
2025-12	44.0	4.0

4.3 User related KPIs

Charging behaviour

Regarding the charging behaviour, Figure 25 shows the average number of EVs connected and charging during the work week in Risø and Bornholm parking lot from November 2024 to January 2026. For Risø parking lot, the average number of connected cars during the day spans from 2 on Monday and Friday, to 1.5 on Thursday, while the average amount of charging cars reaches 1.5 on Monday and is the lowest on Thursday as well, with a value below 1.0. Thursday, of all weekdays seems to be the day with the highest difference between the number of cars connected and charging.

On the contrary, Bornholm parking lot has the highest number of EVs connected on Thursday, this is caused by the different user behaviors in both parking lots. Risø parking lot serve the office employees, while Bornholm parking lot handle school faculty members.

Meanwhile, the figure also shows the average number of total charging session on each day of the week during the analysed period. The total average number of charging session is 785 in Risø parking lot and 207 in Bornholm parking lot. For Risø parking lot, the days with the highest amount of charging session is Monday, followed by Tuesday and Friday. On Wednesday and Thursday there is generally a smaller number of charging sessions. Bornholm parking lot demonstrates the highest number of sessoins on Thursday and the lowest on Tuesday.

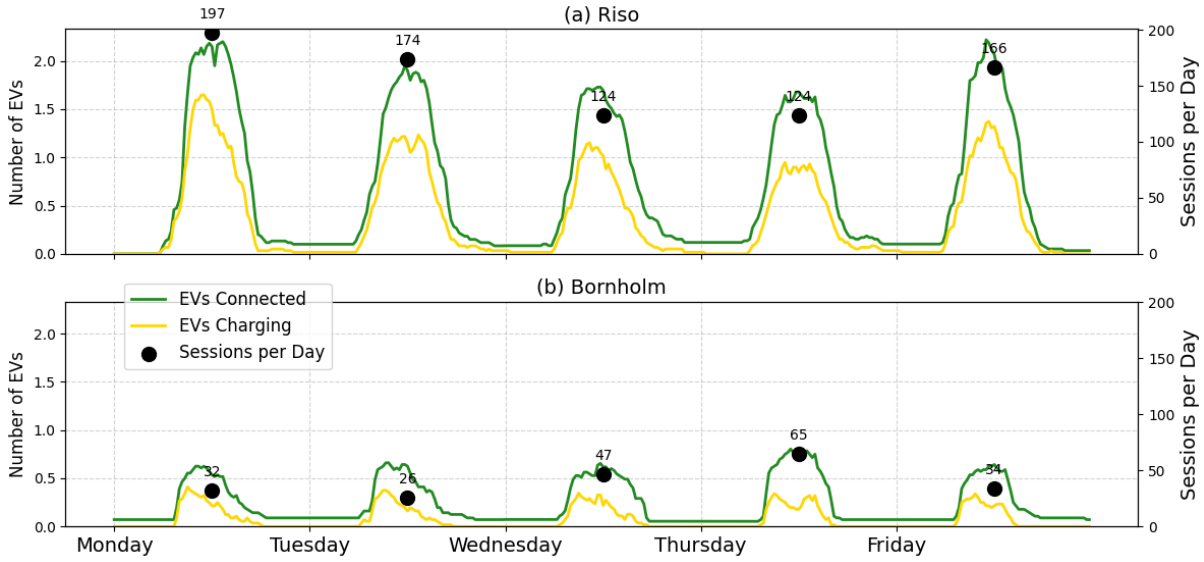

Figure 25: Average number of EVs connected and charging during the work week in Risø parking lot

Figure 26 shows the total hourly distribution of the arrival and departure time during the day. As expected in Risø parking lot, the arrival time of the cars peaks in the early morning, between 8:00 and 9:00, with a second minor peak at 12:00. On the other hand, the departure time gradually incraeses from 9:00 reaching a first peak at 12:00 and having the absolute peak between 15:00 and 16:00 when people working at DTU went home. Bornholm parking lot has significantly high number of sessions apporaching 8 am, which is impacted by the school schdules.

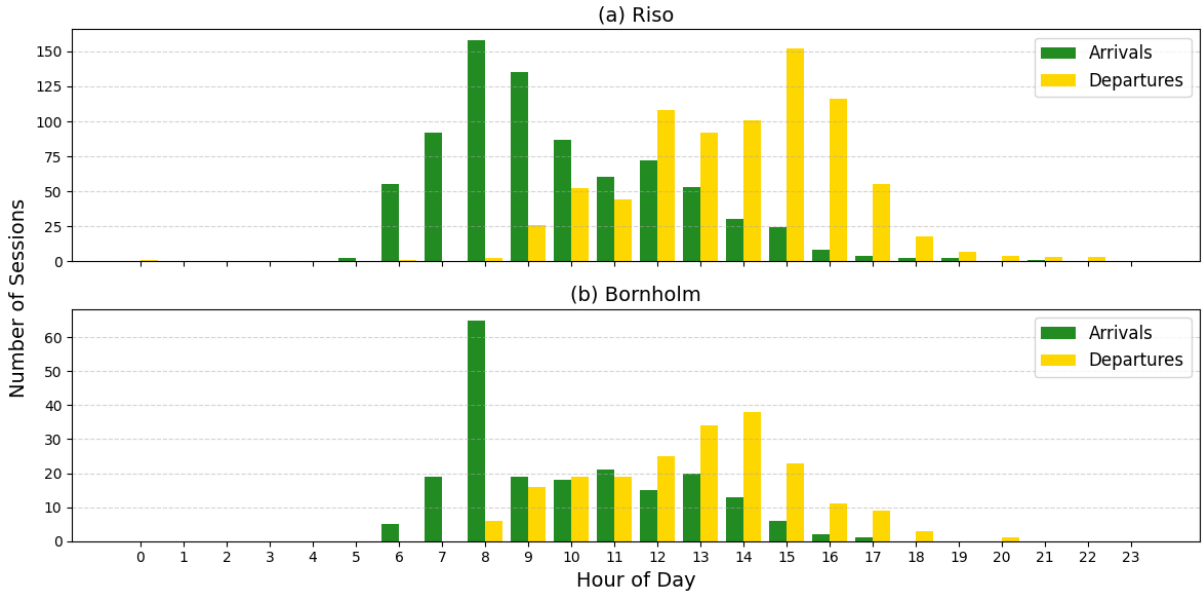

Figure 26: Hourly distribution of the arrival and departure time in Risø parking lot

Figure 27 shows the distribution of the averaged amount of energy charged per session for each weekday. The figure shows the maximum, minimum energy charged, the first quartile, median, third quantile of the average energy charged per each day. For Risø parking lot, the difference in energy charged per charging session seem to be only marginal: the maximum energy charged per session has

a maximum of around 50 kWh, and a minimum of around 2 kWh. However, on Bornholm parking lot, the maximum charged energy reaches 40 kWh on Monday, Tuesday and Friday, whereas Wednesday and Thursday only reach 30 kWh. The reason is that Wednesday and Thursday are the busiest days of the week, which brings additional charging competition of the EVs. Moreover, users on the island of Bornholm don't require as much energy for transportation as the users in the mainland of Denmark.

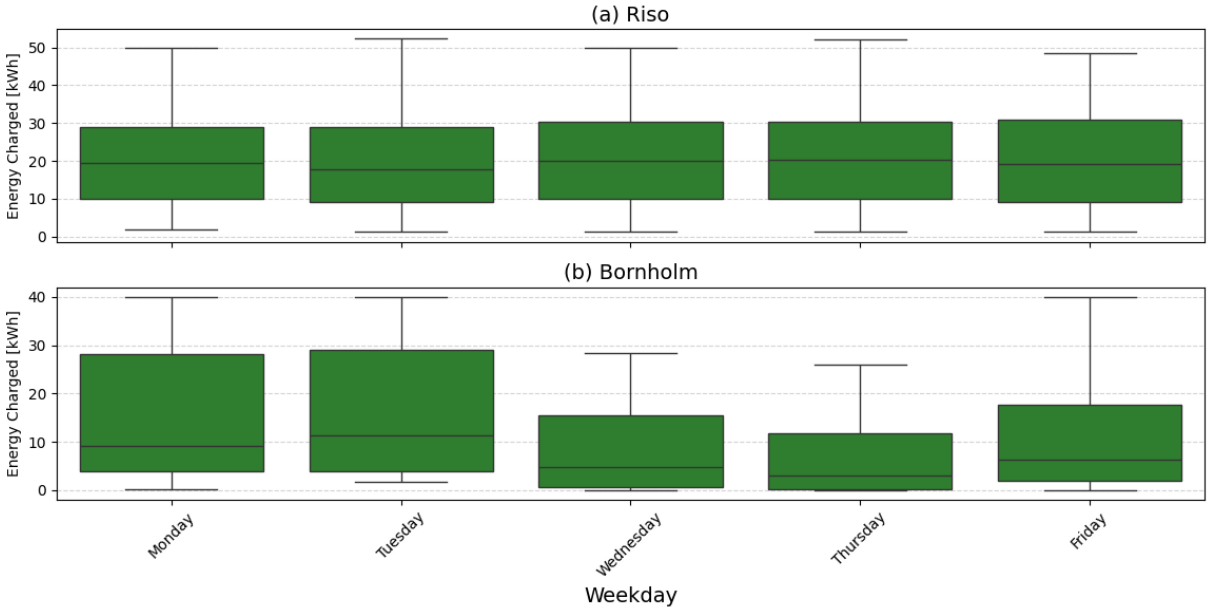

Figure 27: Distribution of the averaged amount of energy charged per session in Risø and parking lot

Figure 28 illustrates a heatmap regarding the average arrival sessions in Risø parking for 2025, it showcases that Monday and Friday are the two busiest days of the week, followed by Wednesday. Tuesday and Thursday, however, have the lowest arrival counts as people preferred to work from home or other offices.

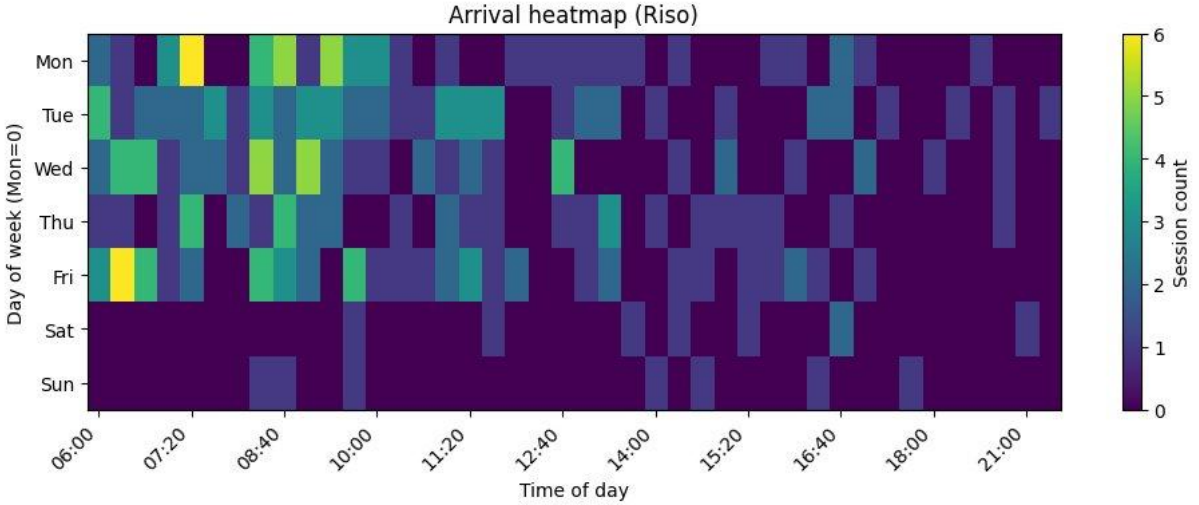

Figure 28: Heatmap of average arrival counts across a week in Risø parking lot

Figure 29 demonstrates the counts and ratio idle time of each charger outlet charging sessions in Risø parking lot in 2025. Nearly half of the charging sessions have an idle duration between 0% to 20%, which represents the limited charging capacity provided by the parking lot. However, there is also about 20% of the sessions where the idle duration is more than 50%, this demonstrates that the users

parked their EVs much longer than their actual needs, which enables the system to offer other beneficial services such as flexibility provision, or RES following to minimize the cost of charge point operator.

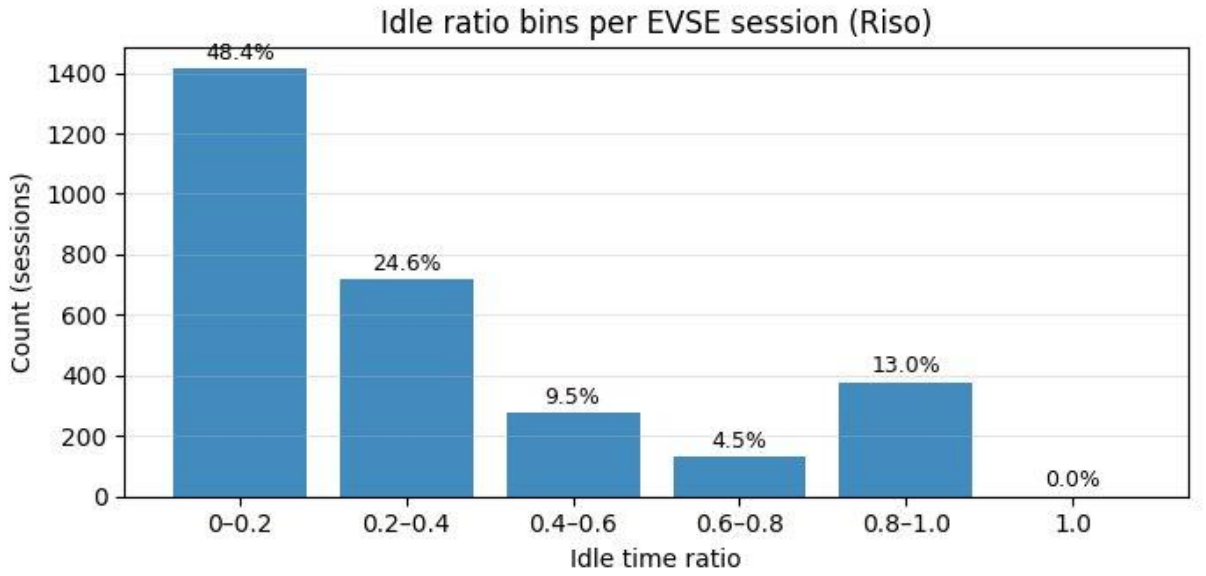

Figure 29: Statistics of idle time of each charging session in Risø parking lot

Figure 30 provides the monthly flexibility indices of Risø parking lot in 2025, especially the second half of the year. The month of May has the highest flexibility in terms of EFI, APFI and MPFI, which attributes to users' preferences of cycling over driving to work when the weather allows. The summer months also have high flexibility indices. On the other hand, the winter months deliver much lower indices, with November as the lowest. Although December is supposed to have the lowest indices, its charging performance is affected by the Christmas vacation period that the employees started their vacation from the second half of the month, hence nobody came requesting charging sessions.

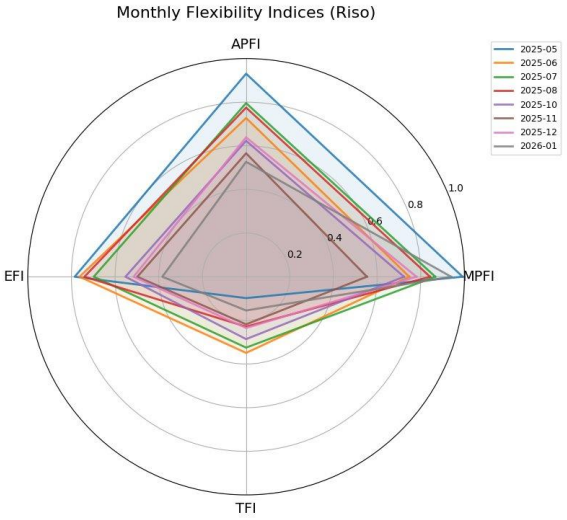

Figure 30: Monthly flexibility indices in Risø parking lot

4.4 Environmental KPIs

Similar to Figure 24, Figure 31 illustrates environmental KPI, which is related to the CO_2 emission of the parking lots with and without accounting for self-consumption from the local PV.

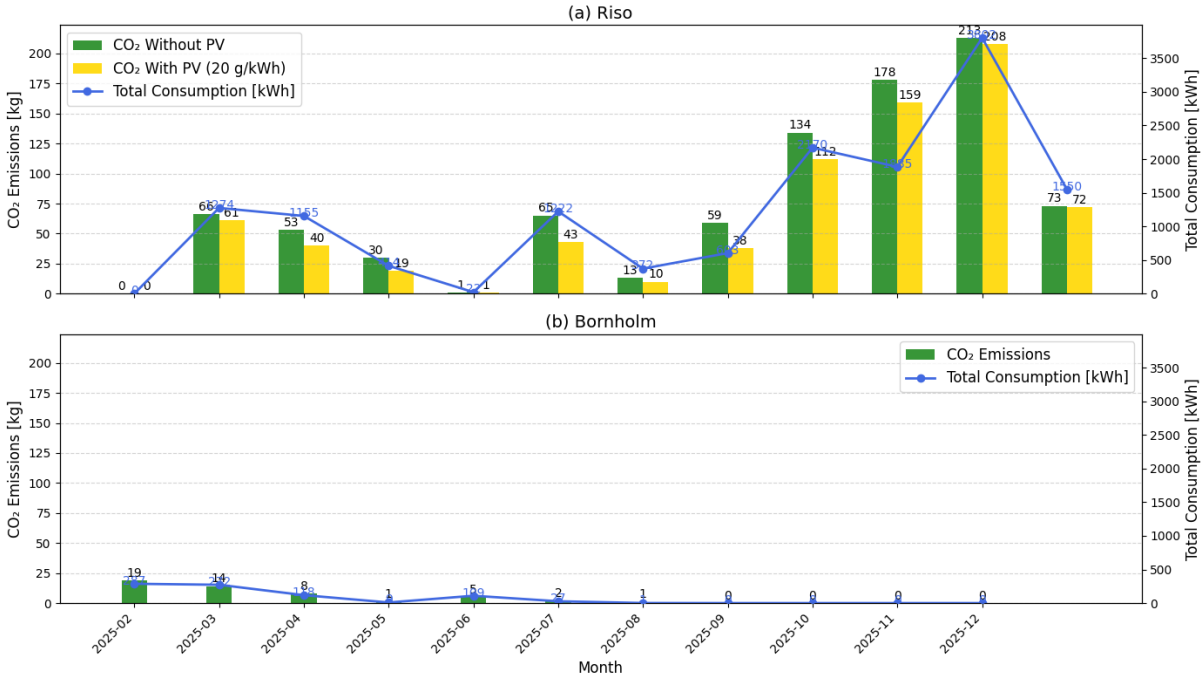

Figure 31: CO_2 emission with and without accounting for the self-consumption from PV in Risø and Bornholm parking lots.

CO_2 emissions are high in cold seasons and low in warm seasons due to the change of users' commuting behaviors. People commuted significantly more with bikes when the weather allows it. However, it can also be observed that during the warm seasons, especially from July to September, the CO_2 emission reduced more with self-consumption from PV, as the PV provided more charging support to the EVs thanks to the sufficient sunshine and longer daytime. This trend also reflects the charging cost demonstrated in Figure 24.

5 Conclusions

The presented document summarizes the results from the implementation and operation of the smart charging system to the demonstration sites in DTU Risø campus and campus Bornholm. The charging infrastructure is accessible in both sites for employees and guests. Both charging clusters are virtually integrated within SYSLAB, a smart energy system lab with distributed units for both production (e.g. PV, wind), consumption (e.g. smart home, heat pumps), and energy storage (e.g. batteries). This provides the unique opportunity to demonstrate the coordination of smart EV clusters with distributed energy resources. A particular focus of the demonstration activities is on load management solutions with distributed control architecture, enabled through the implementation of smart chargers with autonomous control functionality. The chargers were recently installed on the campus and are currently being integrated in SYSLAB and the existing software architecture.

Users of the charging infrastructure start their charging sessions through an app, developed as part of the EV4EU project. The app allows the user to provide inputs, such as the anticipated parking time and the required energy, which enable the load management system to consider user preferences while controlling the overall cluster consumption.

The deliverable presented a detailed overview of the performance of the main smart charging functionalities together with some high-level KPIs designed to showcase the overall statistics of the utilization and of the parking lots. The data coming from all the devices involved is stored in a database. Besides general charging session parameters (charged energy, charging time, connection time), the high-resolution power measurements on both charger and cluster level allow a thorough analysis of test cases. Finally, the deliverable proposes key performance indicators for quantifying the performance and impact of the demonstration activities. The KPIs are organized in four main categories, addressing economical, technical, user-related and environmental impacts. Technical KPI demonstrates high potential flexibility of both parking lots beyond the charging requests from the EVs. Economic and environmental KPIs have showcased that the contribution from PV can significantly reduce the charging cost and CO_2 emissions, especially in warmer seasons when solar energy is sufficient. Finally, user related KPI reveals the user charging behavioural differences in workplace and school scenarios, where people prefer physical attendance in the office on Monday, Tuesday and Friday, whereas the charging behaviors favor Wednesday and Thursday in schools. Statistical idle time and monthly flexibility indices in Risø parking lot also implies high charging flexibility potential.

As a next step, Task 9.5 will provide a description of the lesson learnt from deployment and commissioning of the charging infrastructure at both locations.

6 References

[1] P. Pediaditis et al., “Deliverable D1.3: Regulatory opportunities and barriers for V2X deployment in Europe”, 2023.

[2] M. Zajc et al., “Deliverable D1.4: Business models centred in the V2X value chain”, 2023.

[3] N. Velosa et al., “Deliverable D1.5: V2X Use-cases repository”, 2023.

[4] J. Mateus et al., “Deliverable D2.1 Control Strategies for V2X Integration in Houses”, 2023.

[5] C. Ziras et al., “Deliverable D2.2 Control Strategies for V2X Integration in Buildings”, 2023.

[6] J. Engelhardt et al., “Deliverable D2.3 Optimal management of V2X in parking lots”, 2023.

[7] M. Zajc et al., “Deliverable D5.1 Information Exchange needs to enable different UCs”, 2023.

[8] A. Lekidis, I. Papadopoulos, H. Morais, and A. R. Nunes, “Deliverable D5.2 Standardization gap analysis for new V2X related Business Models”, 2023.

[9] S. Striani, K. Sevdari, M. Marinelli, V. Lampropoulos, Y. Kobayashi, and K. Suzuki, "Wind Based Charging via Autonomously Controlled EV Chargers under Grid Constraints," in Proceedings of 57th International Universities Power Engineering Conference IEEE, 2022.

[10] K. Sevdari, L. Calearo, S. Striani, P. B. Andersen, M. Marinelli, and L. Rønnow, "Autonomously Distributed Control of Electric Vehicle Chargers for Grid Services," in Proceedings of ISGT Europe 2021 IEEE, 2021.

[11] PowerLabDK: SYSLAB. Online: https://www.powerlab.dk/facilities/syslab

[12] A. Malkova, S. Striani, J. M. Zepter, M. Marinelli, and L. Calearo, "Laboratory Validation of Electric Vehicle Smart Charging Strategies," in *Proceedings of 58th International Universities Power Engineering Conference (UPEC 2023)* IEEE, 2023.

[13] X. Cao, S. Striani, J. Engelhardt, C. Ziras, and M. Marinelli, "A semi-distributed charging strategy for electric vehicle clusters," *Energy Reports*, vol. 9, no. 12, pp. 362-367, Oct. 2023.

[14] S. Striani, K. Sevdari, P. B. Andersen, M. Marinelli, Y. Kobayashi, and K. Suzuki, "Autonomously Distributed Control of EV Parking Lot Management for Optimal Grid Integration," in Proceedings of 2022 International Conference on Renewable Energies and Smart Technologies IEEE, 2023.

[15] X. Cao, J. Engelhardt, C. Ziras, and M. Marinelli, "Distributed control of electric vehicle clusters for user-based power scheduling," in *IEEE Transportation Electrification Conference and Expo, Asia-Pacific*, Chiang Mai, Thailand, 2023.

[16] S. Striani, K. Sevdari, L. Calearo, P. B. Andersen, and M. Marinelli, "Barriers and Solutions for EVs Integration in the Distribution Grid," in *Proceedings of 2021 International Universities Power Engineering Conference IEEE*, 2021.

[17] J. Engelhardt, P. B. Andersen, and T. Teoh, "Guidelines – Charging Infrastructure for Truck Depots," European Copper Institute, 2023.

[18] J. Engelhardt, "Reconfigurable Batteries in Electric Vehicle Fast Chargers: Towards Renewable-Powered Mobility," DTU Wind and Energy Systems, 2022.

[19] J. M. Zepter, J. Engelhardt, T. Gabderakhmanova, and M. Marinelli, "Re-Thinking the Definition of Self-Sufficiency in Systems with Energy Storage," in *Proceedings of the 2022 International Conference on Smart Energy Systems and Technologies (SEST),* IEEE, pp. 1–6.

[20] J. Engelhardt, A. Thingvad, J. M. Zepter, T. Gabderakhmanova, and M. Marinelli, "Energy Recovery Strategies for Batteries Providing Frequency Containment Reserve in the Nordic Power System," *Sustainable Energy, Grids and Networks*, vol. 32, p. 100947, 2022.

[21] A. Thingvad, C. Ziras, G. Le Ray, J. Engelhardt, R. Mosbæk, and M. Marinelli, "Economic Value of Multi-Market Bidding in Nordic Frequency Markets," in *Proceedings of International Conference on Renewable Energies and Smart Technologies*, IEEE, 2022.

[22] M. Marinelli, L. Calearo, and J. Engelhardt, "A Simplified Electric Vehicle Battery Degradation Model Validated with the Nissan LEAF e-plus 62-kWh," in *Proceedings of 6th International Electric Vehicle Technology Conference*, 2023.

[23]M. Marinelli, L. Calearo, J. Engelhardt, and G. Rohde, "Electrical Thermal and Degradation Measurements of the LEAF e-plus 62-kWh Battery Pack," in *Proceedings of 2022 International Conference on Renewable Energies and Smart Technologies IEEE*, 2022.
[24]J. Engelhardt, J. M. Zepter, T. Gabderakhmanova, and M. Marinelli, "Energy Management of a Multi-Battery System for Renewable-Based High Power EV Charging," eTransportation, vol. 14, p. 100198, 2022.
[25]A. Bowen, J. Engelhardt, T. Gabderakhmanova, M. Marinelli, and G. Rohde, "Battery Buffered EV Fast Chargers on Bornholm: Charging Patterns and Grid Integration," in *Proceedings of the 57th International Universities Power Engineering Conference (UPEC),* Istanbul, Turkey, 2022.
[26]J. Engelhardt, J. M. Zepter, J. P. Sparresø, and M. Marinelli, "Real-life demonstration of a hybrid EV fast charging station with reconfigurable battery technology enabling renewable-powered mobility," in *Proceedings of the 18th Conference on Sustainable Development of Energy, Water, and Environment Systems (SDEWES),* Dubrovnik, Croatia, 2023.
[27]Cao X, Engelhardt J, Ziras C, Marinelli M. Enhancing phase balance in electric vehicle clusters: a smart charging approach using phase mode switching. In Proceedings of 2024 IEEE PES Innovative Smart Grid Technologies Europe (ISGT EUROPE). IEEE. 2025
[28]Cao X, Engelhardt J, Ziras C, Marinelli M. Grid-friendly operation of EV parking lots: Optimal load management under cluster power and phase unbalance constraints. eTransportation. 2025;26:100458.
[29]Malkova A, Zepter JM, Marinelli M, Korpås M. Which control management strategies are best suited for EV charging stations? A comparison of price optimization and machine-learning approaches. IEEE Transactions on Transportation Electrification. 2026;12(1):1069-1079.
[30]Malkova A, Striani S, Zepter JM, Marinelli M. Distributed Hierarchical Control with Cost Optimization and Priority-Based Dispatch for Workplace EV Charging: A Field Study. Energies. 2025;18(21):5581.
[31]Malkova A, Zepter JM, Marinelli M, Amezquita H, Morais H. Receding horizon optimization for distributed control of electric vehicle charging stations. In Proceedings of 2024 IEEE PES Innovative Smart Grid Technologies Europe (ISGT EUROPE). IEEE. 2025
[32]Striani S, Unterluggauer T, Andersen PB, Marinelli M. Flexibility potential quantification of electric vehicle charging clusters. Sustainable Energy, Grids and Networks. 2024